

Point-by-point responses to the reviewers, including relevant changes made in the revised manuscript

Anonymous Referee #1

The article proposes a method to inverse the rainfall-runoff relationship at the catchment scale to estimate precipitation from runoff. This is an interesting study and the approach may be useful in areas where the estimation of precipitation is difficult, e.g. due to sparse raingauge networks.

I think the article could make a valuable contribution to HESS. However, I have a number of concerns: - the general organization of the paper could be improved, especially the results section

We thank reviewer #1 for his overall evaluation and the constructive comments.

- some explanations and justifications are sometimes too short to fully understand the choices made by the authors in the study,

The manuscript has been substantially changed. As a consequence also explanations and justifications have been revised.

- the validation of the approach should be strengthened, using other test catchments

For the revised manuscript an additional test catchment has been added, to strengthen the validation of the approach.

- there are too many illustrations (24 in total), not all of them appear necessary.

We have removed figures. In total 13 figures remain.

Given these limitations (and other aspects detailed below), I think major revision is needed before the article can be reconsidered for publication.

Detailed comments:

1. P13263,L6: The hypothesis of a closed catchment is quite strong, since there are many catchments where underground water exchanges with deep aquifers or surrounding basins are significant. One implication is that this underground exchange term is neglected later in the study (e.g. in the water balance equation). Does it mean that the approach would not be suitable for basins where there are such underground water losses/gains? This should be further discussed somewhere in the article as a possible limitation of the proposed approach.

It does not make sense to apply the inverse model to leaky catchments or catchments, where a significant part of the runoff is not observed at the gauging site.

Even with a given quantification of the leakage process, the application of a hydrological model would lead to an additional uncertainty difficult to quantify. This is however not necessarily a limitation of the inverse model. Also the application of a forward hydrological model, which needs to be calibrated against runoff observations, will fail or will result in wrong estimates of water balance components. So this limitation would hold for any type of water balance related analysis.

However, we have highlighted this precondition and other limitations concerning the application of the inverse model in section 2.2.1 “Preconditions and limitations of the application of the inverse model” (Line 228).

2. P13263,L24-26: I found this sentence unclear. Could the authors further explain why this approach has limitations that justify the introduction of the new method they purpose?

Kirchner (2009) presented a method to infer catchment rainfall from streamflow fluctuations. The approach is (as stated by Kirchner) limited to catchments, where discharge is determined by the volume of water in storage and which can be characterized as simple first-order nonlinear dynamical systems. The Kirchner (2009) model (when deriving the storage-discharge relationship directly from runoff data) only has a single parameter. In contrast the presented model uses 10 parameters describing several linked storages and accounting for a variety of different runoff components, which of course offer more degrees of freedom and flexibility in describing more complex catchment responses. We have stated this clearly in the revised manuscript (L128-L133).

3. P13265,L19: The equation may give the impression that time steps are considered independently in the method. However, $S(t-1)$ is a function of antecedent rainfalls $R(t-1)$, $R(t-2)$, etc. Maybe this should be stated more clearly.

The state space approach of the model is a first order Markov process: The system states S_t and outputs O_t of the calculation time step depend only on the preceding states S_{t-1} and some inputs I_t and not on the sequences of system states, that preceded it, e.g. S_{t-2} , S_{t-3} , ..., S_{t-n} (see eq. 2 and eq. 3). All information of the sequence of the preceding inputs (I_{t-1} , I_{t-2} , ..., I_{t-n}) is implicitly included in the last relevant system state S_{t-1} . No hysteretic effects are considered in the model and it does not include a

parameter, which introduces a lag effect between inputs and outputs. This has been stated more clearly in the revised manuscript (L201 – L207).

4. P13266,L6: How the upper bound of 50 mm/h was chosen. Is that a general value that can be applied everywhere or is it specific to the study catchment?

50 mm/h is an arbitrary (but reasonable) value. Any reasonable bounds can be applied (L186-L187).

5. P13266,L12-14: Could the authors detail this a bit more? Which disadvantages are they?

A more elegant method to calculate rainfall from runoff is by analytically inverting the equations of a given model, i.e. bringing the rainfall term onto the right side of the equation (Herrnegger, 2013). This is principally possible, but has some disadvantages. The model structure, which was used in Herrnegger (2013) and which can be inverted analytically, differs from the model presented in the manuscript. It does not include interception and routing. Additionally the inversion is not possible in certain periods, since the discontinuities introduced by threshold values lead to non-inversibility in the analytical solution (Herrnegger, 2013). For the forward model used here, the differential equations of the linear reservoirs are solved analytically. An internal time step discretization is included in the model code to guarantee, that the transition between system states above and below the threshold value are solved exactly. This has been stated more clearly in the revised manuscript (L217-L227).

6. P13269,L3-9: I found the choice of the study catchment quite strange. The authors mention at the end of section 2.2 that the method cannot be applied in snow influenced catchment. . . and then they select a test catchment heavily influenced by snow! Consequently, the test of their method can only be done on a short part of the test period where there is no snow influence, which limits the depth of the evaluation of the proposed method (e.g. can it handle seasonal variations in precipitation?). I found this choice unfortunate. Besides, I found that testing the method on a single case study is also limited, since it does not give any information on the transposability

of the method elsewhere. Therefore, I think it would be useful to have at least two study catchments with contrasted climate (and possibly hydrological) characteristics and without snow influence to provide a more comprehensive evaluation. If the authors have a specific interest in the Krems catchment, then it could be kept as an additional case study to show how the method can partly be applied in snow influenced catchments.

Solid precipitation is accumulated without any direct signal on the hydrograph. It is therefore impossible to use the inverse model to estimate solid precipitation. The inverse model can therefore only be used to calculate rainfall in snow-free catchments, or, as in our case, periods, in which runoff is not influenced by snow melt (i.e. summer months of June to September). However, in rainless periods, where it is clear, that snow melt is dominating runoff (e.g. in spring), the inverse model can be used to quantify the snow melt contribution (L249-L251). We have added an additional test catchment for a more comprehensive evaluation, as suggested by the reviewer. Concerning the choice of the catchments, we would like to mention, that it will be hard to find any catchment in Austria (Alpine region), that will not be influenced by snow. Especially in summer time they are frequently influenced by local convective rainfall events, which are difficult to observe with the observation network. Here the inverse model can provide useful information on rainfall.

7. P13270,L4-12: The authors should explain why such a short period is sufficient to test the efficiency of the method, given the known variability of hydroclimatic conditions.

It is clear, that catchments, independent of size, exist, where the application of this particular model structure will fail (e.g. flatland catchments dominated by groundwater). If hydro-meteorological conditions of the catchment change or are different from the calibration period and the forward model (e.g. due to poor parameter estimation, inadequate model structure, wrong representation of the real world prototype etc.) is not able to capture these changes, then again the calculation of rainfall from runoff will fail (as they do for the forward case). Also this limitation has been now stated more clearly (L262-L268).

We have added several simulation experiments (see section 2.3.2), in which we e.g. evaluate the influences of different model parameter calibration periods on the simulation performances.

8. *Section 4: I found this section not well organized. It mixes the presentation of testing methods, criteria and results. I think that all methodological aspects should be presented before the results section, to provide a clearer overview of the testing approach, and then the results section should only detail and discuss the results.*

We have reorganised the sections according to the proposal of reviewer #1.

9. *P13272,L11-13: I found this is not so clear for the year 2007.*

That is correct and has been changed.

10. *P13273,L17: R2 is known to be very sensitive to outlier data. Therefore is it really a well-chosen criterion? MSE is used later. Why these two criteria are necessary?*

We have changed this.

11. *P13273,L19-22: How can this be interpreted? Can the low-pass filter role (smoothing effect) of the catchment be partly responsible for this?*

With temporal aggregation the correlation values generally increase significantly for all combinations. Small differences or timing errors in the 1h-sums are eliminated with temporal aggregation. This is also the case in of the INCA data. This information is now also included in the revised manuscript (L554-L557).

12. *P13273,L27 to P13274,L8: I found this part not really essential.*

The correlation coefficient is a standard criteria frequently used. We also use the correlation coefficient to compare our results to other studies (L574-L589). We therefore think, it is important to keep this evaluation criteria.

13. P13275: *What can be learnt from this?*

It is not clear, to what part of P13275 the question refers to.

14. P13279,L29: *In real time flood forecasting, the target is the future flow, not the past rainfall. So I did not understand why the application of the method would be useful for this application.*

The estimation of areal rainfall leading to extreme flood events is afflicted with major uncertainties. Here the inverse modelling approach can be used as an additional information source concerning the rainfall conditions during extreme events. In this context, it is conceivable to use the inverse model in real-time flood forecasting systems. Here two different applications of the inverse model are conceivable:

1. A frequent problem observed in real-time flood forecasting models with state space formulations is that the system states in the models are biased in such a way that the simulated and observed runoff differ systematically. Methods exist to cope with this problem and to update the system states (e.g. Liu et al, 2012; McLaughlin, 2002). The system states in the inverse model will, at least during driven periods, always guarantee, that the simulated runoff is identical to observations. This fact may be used as a basis for updating system states in the flood forecasting models.

2. At least in Austria, 2 different types of precipitation forecasts are used as input in flood or runoff forecasting models - nowcasting fields (used for forecasts of $t=+1h$ to $t=+6h$) and fields from numerical weather forecasting models (used for $t>+6h$). The nowcasting fields strongly depend on the quality of station observations ($t=0h$), as they are the basis for extrapolation into the future (Haiden et al., 2011). By assimilating the inverse rainfall into the nowcasting system, i.e. to gain additional information on rainfall quantities, it is conceivable that the rainfall estimates of $t=0h$ can be improved. An extrapolation of the improved rainfall fields could therefore improve the nowcasting fields and in consequence the runoff forecasts.

There are however several methodological issues to be solved, before an application in this context is possible. These include the spatial disaggregation of the inverse rainfall and system states in case the flood forecasting models are set up as distributed models or the limitation of the inverse model, when used to calculate rainfall, to snow-free periods. We have addressed this comment in some detail in L712-L737.

15. P13281,L10-11: *I did not understand this sentence.*

Percolation from the soil layer was initially calculated using a linear reservoir with a time-invariant parameter KBF. With the additional parameter PEX2, KBF becomes time-variant, calculated as a function of soil moisture (L770-L774).

16. Table 1: *What is the source of these values? Any reference?*

References have been added to the table (Tab. 1).

17. Table 3: *Should fluxes not be expressed as depth per time step?*

The fluxes represent sums over the time-step. This information has been added (Tab. 3).

18. Figure 1: *BWI should appear in the first store*

Figure 1 has been changed.

19. Figure 2: *This is quite classical. Is it really useful here?*

We have removed this figure.

20. Figures 4 and 5: *Could these two figures not be merged?*

We have removed Figure 5.

21. Figure 7. *Remind in the caption that only a few months are used each year.*

We have added this information to the first tables, in which performance criteria are shown.

22. Figure 8: *It is always nice to have hydrographs shown, but I found the added value of this figure is rather limited.*

We have changed the hydrographs. The intention is not necessarily to show details, but the general runoff characteristics of the catchments. Additionally the hydrographs are used as a basis for explanations of results, e.g. in section 4.3.1.

23. Figure A1: *Is this figure useful, given it is not really commented in the text?*

The figure has been removed.

Anonymous Referee #2

General comments:

The paper by Herrnegger et al. presents a method to derive estimates of rainfall from runoff and potential evapotranspiration by inverting a rainfall-runoff model. The paper is clearly written and well presented, it deals with a very interesting topic and the authors have covered several important issues related to the method presented including the impact of model initialisation, model calibration and validation. However, we believe that the method requires significant improvements before the paper can be accepted for publication. Three points require the author's attention:

We thank reviewer #2 for his overall evaluation and the constructive comments.

- *Inversibility of the state-space equation: the method presented by the author is based on the inversion of the state-space equation presented in Equation 4. The authors have not fully explored the fact that the relationship may not be invertible in certain conditions. They have mentioned invertibility problems related to snow pack and distributed modelling in section 2.2.1. However, we believe that this problem is far more common than suggested by the authors, due to the two following issues:*

- *Thresholds: many rainfall-runoff model structures use threshold functions to process input data. For example the COSERO model relies on three min/max operators in equation A1, A2, A3 and A5. These functions introduce discontinuities in the relationship between rainfall and runoff preventing an inversion algorithm to be applied. A simple example can be given with the interception reservoir of the COSERO model: in equation A1, $BW I_t = 0$ whatever value of rainfall R_t is chosen such as $R_t < ET P_t - BW I_{t-1}$, as a result the state space equation related to the particular state $BW I_t$ is not invertible for low rainfall values. This example illustrates the difficulty of inverting rainfall-runoff models during low rainfall periods or in high evaporation catchments.*

The equations in the appendix have been partially revised. Thresholds in the model do not limit the inversion. The differential equations of the linear reservoirs are solved analytically. An internal time step discretization is included in the code, to guarantee, that the transition between system states above and below the threshold value is solved exactly. A3, representing the soil layer, does include a min() operator for

estimating the ratio between actual and potential evapotranspiration as a function of soil water content. This is however not a limiting factor for the inversion, since this factor is a function of the preceding soil state $BW_{0,t-1}$, which is known. Only 50% of rainfall is used as input into the interception storage BWI. By assuming that the other 50% are always throughfall, eq. A1 and A2 also do not limit the inversion, since a continuous signal through the whole model cascade is guaranteed. Note, that in our case the 50% is a fixed value, but could be an additional model parameter (as long the lower limit is larger than 0%). We have added this information to the manuscript (L224-227 and Appendix).

- *Delayed responses:* Equation 1 assumes that the runoff at time step t is a function of inputs during the same time step (i.e. R_t). However, many rainfall-runoff model structures (e.g. HBV with the MAXBAS parameter) introduce a lag effect between inputs and outputs. As a result, Equation 1 could be rewritten $Q_t = f(R_t, R_{t-1}, R_{t-2}, \dots, R_{t-n}, ET P_t, S_{t-1}, \theta_j)$. In this case, it is not clear how the inversion algorithm works because it has to deal with rainfall values at several time steps simultaneously.

The state space approach of the model is a first order Markov process: The system states S_t and outputs O_t of the calculation time step depend only on the preceding states S_{t-1} and some inputs I_t and not on the sequences of system states, that preceded it, e.g. $S_{t-2}, S_{t-3}, \dots, S_{t-n}$ (see eq. (2) and eq. (3)). All information of the sequence of the preceding inputs ($I_{t-1}, I_{t-2}, \dots, I_{t-n}$) is implicitly included in the last relevant system state S_{t-1} . No hysteretic effects are considered in the model and it does not include a parameter, which introduces a lag effect between inputs and outputs. This has been stated more clearly in the revised manuscript (L201 – L207).

Overall, we believe that the inversion method as presented by the authors is possible in many situations, but requires a clear definition of feasibility conditions. This point could be explored in the synthetic experiments. In addition, it is clear that inversion is impossible in certain conditions (e.g. dry spells, high evaporation catchments,...), it would be useful for the authors to provide more context on the intended use of the method to judge if these limitations pose a real challenge to be explored further.

We have added the section 2.2.1, in which limitations and preconditions in the application of the inverse model are clearly stated. The virtual experiments

however show that the inversion is possible (see section 4.1 and Fig. 5 as an example).

- *Impact of rainfall-runoff model structure: The method presented by the authors heavily relies on a single rainfall-runoff model (COSERO). As a result, it is not possible to differentiate the impact of the inversion method itself from the one of the rainfall-runoff model. We suggest adding at least another rainfall-runoff model and check the link between the performance of the forward model and results obtained by the inversion method.*

A comparison of inverse rainfall estimates from a different model structure for the two catchments with our results would be of interest, in order to check the possible links between the performance of the forward model and the results obtained by the inversion method. We have highlighted this fact in section 5 (L740-L743). Adding an additional model structure to the analysis is clearly beyond the scope of this already comprehensive manuscript. Our results suggest that there is a link between the model performance of the forward model and the inverse rainfall simulations.

- *Limited scope of the catchment dataset: all results presented cover a single catchment of 38 km² for a period of 3 years. It is extremely difficult to generalize this setup to other hydrological conditions and we urge the authors to consider a larger number of catchments with longer simulation periods. Problems like non-stationarity, poor data quality, prolonged spin-up periods and model biases need to be factored in the results for the method to become relevant to the hydrological community. We are aware that getting hourly data is not simple for large catchment samples, but the study could be performed at the daily timestep with equally interesting outcome.*

4 years of data are available (see section 3.2/3.3 of the manuscript). We have added an additional test catchment for a more comprehensive evaluation, as suggested by the reviewer. No substantial differences in the results are found between the two study areas.

It is clear, that catchments, exist, where the application of this particular model structure will fail (e.g. flatland catchments dominated by groundwater). If hydro-meteorological conditions of the catchment change or are different from the calibration period and the forward model (e.g. due to poor parameter estimation, inadequate model structure, wrong representation of the real world prototype etc.) is not able to capture these changes, then again the calculation of rainfall from runoff will fail (as they

do for the forward case). This is now also clearly stated in section 2.2.1. We additionally set up several simulation experiments (see section 2.3.2 /3.3. and Table 5) to evaluate the influences of (i) different model parameters due to different calibration periods and lengths, (ii) different runoff observations and (iii) different parameter optimisation data basis on the simulated runoff and rainfall (see section 4 for the results).

Detailed comments are provided in the following section.

2 Specific comments

1. Page3 Line9, “Errors are considerably lower compared to rainfall”: This is certainly true, however the authors process the streamflow data via a non-linear inverse model that could easily magnify streamflow errors by several order of magnitude. I suggest a comment on this point.

We have added a simulation experiment, with the aim to evaluate the influence of possible streamflow errors (see section 2.3.2 / Exp4 in Table 5 / results section) on the inverse rainfall.

2. Page6 Eq 5 : Please add the objective function that was used in the root-finding algorithm (e.g. squared error). I presume that equation 5 is essentially a stop criteria for the algorithm.

Equation 5 is the objective function used in the root-finding algorithm. This has been stated more clearly in the text (L190).

3. Page7 L17, “Reservoir without memory” : I don’t understand this statement. Please clarify and give examples.

The statement has been changed. Additionally, the section concerning the limitations of the application of the inverse model have been substantially revised (see section 2.2.1).

4. Page7 L22, “small errors ... can be amplified” : This statement confirms that small errors in streamflow data can back propagate within the inverse model and heavily influence the rainfall estimates. We suggest adding an experiment testing this assumption.

We have added a simulation experiment, with the aim to evaluate the influence of possible streamflow errors (see section 2.3.2 / Exp4 in Table 5 / results section) on the inverse rainfall.

5. Page13 L10, “model performance expressed by the correlation coefficient” : Please add also bias of model simulations. Bias is sometimes difficult to re-produce, especially if the model is calibrated with NSE objective function.

Thank you for the suggestion. The bias has been added (see Table 6).

6. Page20 L4 : What is the effect of $BW I_t$ to the rest of the model? I can't see it mentioned in subsequent equations. Please clarify.

The equations in the Appendix have been revised and further explanations have been added.

7. Page20 L6 : Is it really $PEX2$ or $f(PEX2)$ that should be mentioned in equation 2 with f the function displayed in Figure A1? Please clarify.

$f(PEX2)$ is correct and has been changed.

8. Page26 Tab 2 : I presume that the upper and lower values of the TAB and TVS parameters vary with the time step. Otherwise, we could get α and β parameters greater than 1, which could lead to negative values of BW_j . Please clarify.

The values of α and β and vary with modelling time step and represent smoothing functions of the linear reservoirs.

9. Page31 Figure 9 : Scatter plots are extremely misleading for flow data because of the high concentration of point in the lower left corner. Please change both axis to log scale to get a better distribution of values along the axis.

We have removed Figure 9.

10. Page33 Figure 11: Same comment than #9

We have removed Figure 11.

Anonymous Referee #3

General comments:

This manuscript claims that one can use a calibrated rainfall-runoff model to "predict" rainfall from runoff time series, by using a search algorithm to find, hour by hour, the rainfall rate that best fits the observed runoff.

This result is somewhat surprising, because mathematically speaking one would expect the inversion of a multi-compartment model to be ill-posed (because different rainfall inputs at different times, and different combinations of storage levels in the different compartments, should lead to the same discharge), and possibly also mathematically unstable. In that respect the results claimed here are intriguing.

The state space approach of the model is a first order Markov process: The system states S_t and outputs O_t of the calculation time step depend only on the preceding states S_{t-1} and some inputs I_t and not on the sequences of system states, that preceded it, e.g. S_{t-2} , S_{t-3} , ..., S_{t-n} (see eq. (2) and eq. (3)). All information of the sequence of the preceding inputs (I_{t-1} , I_{t-2} , ..., I_{t-n}) is implicitly included in the last relevant system states S_{t-1} . So, the model state and the output at time t depend only and exclusively on the previous state S_{t-1} , the inputs I_t and parameters θ_i . Given ET_{pt} , S_{t-1} and θ_i , there is only one single input I_t , which results in an output O_t (eq. (3)). The inverse rainfall and resulting runoff are therefore solely a function of the initial cold system states. The influence of the initial cold system states on the inverse rainfall calculation are analysed in the results section. This information has been added in section 2.1 and 2.2 in the revised manuscript.

However, the manuscript does not make a convincing case for its central claims, in several important respects.

1. First of all, the manuscript claims to "predict" rainfall from runoff, but it can only do this at sites where it already has extensive rainfall data to calibrate the model with. This leaves the reader wondering: how can we "predict" a

*rainfall time series if, in order to do so, we must already *have* the rainfall time series so that we can calibrate the model?*

It is actually the same situation when hydrologist forward-predict runoff. In order to do so we need rainfall and runoff time series to calibrate the model. This is not only the case in hydrological models but environmental models in general. In the revised manuscript we have set up different simulation experiments, in order to evaluate the influence of the calibration period and length on the simulation results (see section 2.3.2 / Table 5 / results).

*2. The manuscript claims that this method will be useful for generating improved estimates of mean areal rainfall. The manuscript presents no convincing evidence to support this claim. Indeed, unless one already *has* good estimates of mean areal rainfall, one will be calibrating the model with incorrect rainfall data, with potentially serious consequences for the calibrated parameter values and the resulting "predictions" of rainfall from runoff.*

See above answer to referee #3.

3. This is a 12-parameter model. More than two decades ago, Jakeman and Hornberger (1993) showed that typical rainfall-runoff time series were unable to constrain the parameters of even a two-compartment, four-parameter hydrologic model. A 12- dimensional parameter space is absolutely vast compared to a four-dimensional parameter space (as a simple illustration, a 4-dimensional cube has 16 corners, but a 12-dimensional cube has 4096 corners). Rampant equifinality is virtually guaranteed in such a model. The manuscript gives no indication of any awareness of the equifinality problem, and no indication that anything has been done to deal with it, or even to assess how serious it is.

For our model 10 parameter where optimized. 2 parameter values where assigned a priori.

For the revised manuscript we additionally set up several simulation experiments (see section 2.3.2 /3.3. and Table 5) to evaluate the influences of (i) different model parameters due to different calibration periods and lengths, (ii) different runoff observations and (iii) different parameter optimisation data

basis on the simulated runoff and rainfall (see section 4 for the results). The simulation experiments do not allow a systematic analysis of parameter uncertainty or the assessment of equifinality. This is not the aim of this paper. The simulation experiments however enable a first assessment of the robustness of the results. That is to show the forward and inverse model performance, when the conditions are different from the conditions the model has been calibrated against or if different driving inputs are used (L309-L314 in the revised manuscript).

In the conclusions we highlight, that the influences and uncertainties in the inverse rainfall, which arise from different model parameters should be analysed systematically (738-740). The topic is not in the scope of this manuscript and must be dealt with in future research.

4. The only validation that is presented here consists of calibrating the model for 2006, 2007, and 2008, and then running it without calibration in 2009. It should be recognized that this is an extremely weak test, because the model is being tested against one year that is nearly identical to the three other years that it was already calibrated with (at least I believe this to be the case, but the figures present almost no information about the validation data, whereas the calibration data are presented in much greater detail). This problem was already pointed out over a decade ago by Seibert (Nordic Hydrology 34, 477-492, 2003) in the context of rainfall-runoff modeling. Seibert observed that models typically give good fits to calibration data, and also to "validation" data that is virtually the same as the calibration data, but then fail spectacularly whenever they are tested against data that are somewhat outside the calibration conditions (that is, whenever the "predictions" are really predictions, rather than fits to existing data or functionally equivalent data sets).

This problem becomes more acute as models become more parameterized; thus it is likely to be a particularly serious problem in the present case. The manuscript must demonstrate that the proposed approach can predict rainfall under conditions that are substantially different from the conditions the model has already been calibrated against.

For the revised manuscript additional simulation experiments (see section 2.3.2 /3.3. and Table 5) were set up, to evaluate the influences of different model parameters due to different calibration periods and lengths. That is to show the forward and inverse model performance, when the conditions are different from the conditions the model has been calibrated against. An additional test catchment has been added, to strengthen the validation of the approach (see section 3.1 and results section).

5. The abstract claims that "To verify the existence, uniqueness and stability of the inverse rainfall, numerical experiments with synthetic hydrographs as inputs into the inverse model are carried out successfully." Absolutely no evidence to support this statement is provided; the reader is referred instead to the first author's Ph.D. thesis. What was done, apparently, was to put precipitation numbers into the forward model to generate streamflow, then to put exactly those streamflow numbers into the inverse model to generate precipitation again. This does not demonstrate stability, at least in any sense that really matters. It does not test, for example, whether small errors in the streamflow numbers will generate big errors in the inferred precipitation (which would seem to be likely, particularly at short time scales). It also does not test the even more important question of how structural errors in the model (which must exist, because no model is an exact copy of the real hydrological system) will affect the accuracy of the rainfall "predictions".

The section of the virtual experiments has been reorganised and exemplary results are shown. Additionally a simulation experiment has been added, with the aim to evaluate the influence of possible streamflow errors (see section 2.3.2 / Exp4 in Table 5) on the inverse rainfall. A comparison of inverse rainfall estimates from a different model structure for the two catchments with our results would be of interest. We have highlighted this fact in section 5 (L740-L743). Adding an additional model structure to the analysis is clearly beyond the scope of this already comprehensive manuscript.

5. Figures 10 and 16 show impressive-looking cumulative rainfall curves, which appear to show very close correspondence between the model results and two data sets. It is important to recognize that this proves nothing except that the model conserves mass, and thus that the amount of rainfall that is

predicted to go into the model is consistent with the runoff that is measured going out of it (plus evapotranspiration, about which surprisingly little is said).

The large difference between cumulative rainfall and runoff curves (which have been added in the revised manuscript) highlight the importance of actual evapotranspiration (ETa) in the catchments (Fig. 9 and Fig. 10). Over 60 % of rainfall are lost to evapotranspiration in the Schlieffau catchment. Nearly 45 % of rainfall are lost to the atmosphere in the Krems catchment. ETa from the model reflects the complex interplay and temporal dynamics of the system states of the different parts of the model. If the model would not capture ETa adequately, the cumulative rainfall curves would not follow the observations so closely. Information about this facts have been added to revised manuscript (L517-L531).

6. At a shorter time scale, the same effect is likely to be behind the apparent increase in goodness-of-fit, shown in Figure 11, as rainfall estimates are averaged over longer intervals, from 1 hour to 6 hours to 24 hours. Because the model must conserve mass, the integrated inputs and outputs must be equal, over timescales than the storm response timescale (that is, the timescale that changes in storage can allow inputs and outputs to diverge substantially). Thus as the averaging interval becomes longer, the inputs and outputs must match more closely.

As stated above, the mechanisms leading to a “correct” mass balance are more complex than suggested by referee #3.

7. In this respect, it is interesting to compare the results presented in Figure 11 with the much simpler method of Kirchner (2009). In the current manuscript, the inverse model predicts one-hour precipitation with an r -squared of 0.24, whereas Table 4 of Kirchner (2009) shows r -squared values of 0.66 ($r=0.81$) and 0.77 ($r=0.88$) for one-hour rainfall predictions at his two sites. Most importantly, in that approach, predictions are really predictions, because they are not calibrated against any precipitation measurements.

A comparison of correlation and bias values from Kirchner (2009) and Krier et al. (2012) and possible explanations for the differences have been added to the revised manuscript (L574-L589, L607-610). We have highlighted in the conclusion that the application of a different model structure in our test areas are topics of future work (L740-L743).

Marked-up manuscript

From runoff to rainfall: ~~I~~inverse rainfall-runoff modelling in a high temporal resolution

M. Herrnegger¹, H.P. Nachtnebel¹ and K. Schulz¹

[1] {Institute of Water Management, Hydrology and Hydraulic Engineering, University of Natural Resources and Life Sciences, Vienna, Austria}

Correspondence to: Mathew Herrnegger (mathew.herrnegger@boku.ac.at)

Abstract

This paper presents a novel technique to calculate mean areal rainfall in a high temporal resolution of 60-min on the basis of an inverse conceptual rainfall-runoff model and runoff observations.

Rainfall exhibits a large spatio-temporal variability, especially in complex alpine terrain. Additionally, the density of the monitoring network in mountainous regions is low and measurements are subjected to major errors, which lead to significant uncertainties in areal rainfall estimates. The most reliable hydrological information available refers to runoff, which in the presented work is used as input for an inverted rainfall-runoff model. Thereby a conceptual, HBV-type model is embedded in an iteration-root finding algorithm. For every time step a rainfall value is determined, which results in a simulated runoff value that corresponds to the observation.

~~To verify the existence, uniqueness and stability of the inverse rainfall, numerical experiments with synthetic hydrographs as inputs into the inverse model are carried out successfully. The application of the inverse model with runoff observations as driving input, also evaluating different model parameter sets, is performed applied for to the Schlieffau and Krems catchments (38.4 km²), situated in the northern Austrian Alpine foothills. Generally, no substantial differences between the catchments are found. Compared to station observations in the proximity of the catchments, the inverse rainfall sums and time series have a similar goodness of fit, as the independent INCA rainfall analysis of Austrian Central Institute for Meteorology and Geodynamics (ZAMG). Compared to observations, the inverse rainfall estimates show larger rainfall intensities. Numerical experiments show, that cold state conditions in the inverse model do not influence the inverse rainfall estimates, when considering an adequate spin up time. The application of the inverse model is a feasible-promising approach to obtain improved estimates of mean areal rainfall. These can be used to enhance interpolated rainfall fields, e.g. for the~~

Formatiert: Deutsch (Österreich)

32 estimation of rainfall correction factors, the parameterisation of elevation dependency or the
33 application in real-time flood forecasting systems. The application is limited to (smaller)
34 catchments, which can be represented with a lumped model setup and to the estimation of liquid
35 rainfall.
36

1 Introduction

The motivation for the inverse model concept presented in this paper comes from practical hydrological problems we encountered. Some years back we set up rainfall-runoff models for different alpine rivers (e.g. Stanzel et al., 2008; Nachtnebel et al., 2009a, 2009b, 2010a or 2010b). In the course of these projects, we were confronted with massive errors in the precipitation input fields. This is a known problem, especially in alpine environments. Although the temporal dynamics in the runoff simulations were captured quite well, we observed significant mass balance errors comparing between observed and simulated runoff were found. We could be excluded, that erroneous evapotranspiration calculations –were biasing the results (Herrnegger et al., 2012). In the HYDROCAST project (Bica et al., 2011) we tested different precipitation interpolation and parameterisation schemes by using the ensemble of generated inputs for driving a rainfall-runoff model and comparing the simulated runoff time series with observations. In essence, the results showed, that no significant improvements could be made in the runoff simulations and that the information on the precipitation fields is strongly determined and limited by the available station time series. The only additional information available concerning the precipitation of a catchment is the runoff observation. The main aim is therefore to present a proof-of-concept for the inversion of a conceptual rainfall runoff model. That is to show, that it is possible to use a widely applied model concept to calculate mean areal rainfall from runoff observations.

Areal or catchment rainfall estimates are fundamental for many hydrological problems, as they represent an essential input for modelling hydrological systems. They are however subject to manifold uncertainties, since it is not possible to observe the mean catchment rainfall itself (Sugawara, 1993; Valéry et al., 2009). Catchment rainfall values are therefore generally estimated by interpolation of point measurements, sometimes incorporating information on the spatial rainfall structure from remote sensing, e.g. radar (e.g. Haiden et al., 2011). Measurement, sample and model errors can be identified as sources of uncertainty. Point observations of rainfall, which are the basis for the calculation of mean areal rainfall values, are error inflicted (Sevruk, 1981, 1986; Goodison et al., 1998; Sevruk and Nespor, 1998; Seibert and Moren, 1999; Wood et al., 2000; Fekete et al., 2004). Occult precipitation forms like fog or dew are frequently ignored. Although not generally relevant, this precipitation form can be a significant contribution to the water budget of a catchment (Elias et al., 1993; Jacobs et al., 2006; Klemm and Wrzesinsky, 2007). The highest systematic

measurement errors of over 50 % are found during snowfall in strong wind conditions. Other sources of systematic measurement errors and their magnitudes are listed in Tab-le 1.

➔ Approximate location of Tab. 1

In complex terrain the rainfall process is characterised by a high temporal and spatial variability. Especially in these areas the density of the measurement network tends to be low, not capturing the high variability and leading to sample errors (Wood et al., 2000; Simoni et al., 2011; de Jong et al., 2002). Further uncertainties arise in the interpolation of catchment scale rainfall from point observations. Systematic and stochastic model errors of the regionalisation methods can be identified-~~(model errors)~~. Systematic model errors can arise during the regionalisation of rainfall in alpine areas, when e.g. the elevation dependency is not considered (Haiden and Pistotnik, 2009). Quantitative areal rainfall estimates from radar products are, although they contain precious information on the rainfall structure, still afflicted with significant uncertainties (Krajewski et al., 2010; Krajewski and Smith, 2002). A general magnitude of overall uncertainty, which arises during the generation of areal rainfall fields, is difficult to assess, as different factors, e.g. topography, network density or regionalisation method, play a role.

Errors in runoff measurements are far from negligible (Di Baldassarre and Montanari, 2009; McMillan et al., 2010; Pappenberger et al., 2006; Pelletier, 1987). When applying the rating-curve method for estimation of river discharge the uncertainties are a function of the quality of the rating curve and the water level measurements. The quality of the rating curve depends on (i) the quality and stability of the measured cross-section over time, (ii) the representativeness of the velocity measurements and (iii) the influence of steady and unsteady flow conditions. According to literature the overall uncertainty, at the 95 % confidence level, can vary in the range of 5% - 20% (Di Baldassarre and Montanari, 2009; Pelletier, 1987). Although it can be expected, that the measurement error will certainly be large during flood events due to its dynamic features, the errors are considerable lower compared to rainfall measurements and to the uncertainties introduced, when calculating mean areal rainfall. It must however be assumed, that transboundary flows and groundwater flows around the gauging station are ~~small and can therefore be neglectednegligible~~. ~~In this paper we therefore present and explore a method to estimate catchment rainfall from runoff observations in a high temporal resolution of 60 min on the basis of a HBV-type conceptual hydrological model.~~

101 A classical application of hydrology, the problem of reproducing observed runoff with
102 meteorological forcings as input through a formalised representation of reality, is a forward or
103 direct problem. Two inverse problems can be identified with the forward problem (Groetsch,
104 1993):

105 1. Causation problem: Determination of input I (=cause), with given output O (=effect)
106 and given model K, including model parameters θ (=process)

107 2. Model identification problem: Determination of model K, given input I and output O

108 The model identification problem can be divided into (i) the problem of identifying the model
109 structure itself and (ii) the determination of model parameters that characterise the system
110 (Tarantola, 2005). The focus in this contribution lies in solving the causation problem, i.e. in
111 the determination of rainfall input from runoff, with a given model structure and parameters.
112 In the following, the model, which calculates mean catchment rainfall values from runoff, will
113 be called inverse model. The conventional model, which uses rainfall and potential
114 evapotranspiration as input to calculate runoff, will be called forward model.

Formatiert: Schriftart: Kursiv

Formatiert: Schriftart: Kursiv

115 Runoff from a closed catchment is the integral of rainfall over a certain period, considering
116 evapotranspiration losses and water storage characteristics within the catchment. Therefore,
117 runoff observations can be used to derive information on rainfall. This has been done in
118 several studies, e.g. Bica et al., 2011; Valéry et al., 2009, 2010; Ahrens et al., 2003; Jasper
119 and Kaufmann, 2003; Kunstmann and Stadler, 2005 or Jasper et al., 2002. The common basis
120 of these studies was to indirectly gain information on catchment rainfall by comparing
121 simulated runoff results with observations. Hino and Hasabe (1981) fitted an AR
122 (autoregressive) model to daily runoff data, while assuming rainfall to be white noise. By
123 inverting the AR model they directly generated time series of rainfall from runoff. Vrugt et al.
124 (2008) and Kuczera et al. (2006) derived rainfall multipliers or correction factors from stream
125 flow with the DREAM- and BATEA-methods, these methods however being computationally
126 intensive. In a well-received study, Kirchner (2009) analytically inverted a single-equation
127 rainfall-runoff model to directly infer time series of catchment rainfall values from runoff.
128 The Kirchner model (when deriving the storage-discharge relationship directly from runoff
129 data) only has a single parameter and does not need rainfall as driving input for calibration.
130 Rainfall data is however needed for the determination of rainless periods for the estimation of
131 the sensitivity function. -Krier et al. (2012) applied the model of Kirchner (2009) to 24 small
132 and mesoscale catchments in Luxembourg to generate areal rainfall. No systematic

133 differences in the quality of the rainfall estimates are found between different catchment sizes.
134 In periods with higher soil moisture the rainfall simulations show a higher performance,
135 which is explained by the fact, that wet catchments are more likely to react as simple
136 dynamical systems. The parsimonious approach of Kirchner (2009) is ~~however limited to~~
137 ~~catchments, in which discharge is determined by the volume of water in storage. However~~
138 ~~limited to catchments, where discharge is determined by the volume of water in a single~~
139 ~~storage and which can be characterized as simple first-order nonlinear dynamical systems.~~
140 Also due to the larger number of model parameters, ~~describing several linked storages,~~
141 ~~accounting for a variety of different runoff components, HBV-type conceptual models and~~
142 ~~offer thus~~ higher degrees of freedom and flexibility in the calibration procedure. ~~They can,~~
143 ~~HBV-type conceptual models in contrary consequence, can~~ be applied to catchments with a
144 wider range of runoff characteristics (Bergström, 1995; Kling et al., ~~2014~~2015; Kling, 2006;
145 Perrin et al., 2001). Therefore, in this study, the conceptual rainfall-runoff model COSERO
146 (Nachtnebel et al., 1993; Eder et al., 2005; Kling and Nachtnebel, 2009, Herrnegger et al.,
147 2012; Kling et al., ~~2014~~2015, among others), which in its structure is similar to the HBV-
148 model, is used as a basis for the inverse model. The COSERO model has been frequently
149 applied in research studies, but also engineering projects (see Kling et al., ~~2014-2015~~ for
150 details).

151 This paper is organized as follows: Following this introduction the methods-section describes
152 the conventional conceptual rainfall-runoff model (forward model), ~~and the inverse model,~~
153 ~~including the preconditions and limitations of their application. and the v~~The concept of
154 virtual experiments to ~~test the inverse model and to verify-analyse~~ the existence, uniqueness
155 and stability of the inverse rainfall simulations ~~are presented. Additionally, the setup of~~
156 ~~different simulation experiments, e.g. to evaluate the influence of differing calibration periods~~
157 ~~or possible runoff measurement errors on the simulations, are explained.~~ The inverse model is
158 applied to ~~a two headwater catchments in the foothills of the northern Austrian Alps, with~~
159 ~~differing hydro-climatic and physical conditions in the foothills of the northern Austrian Alps.~~
160 The catchments and the data base, ~~including the calibration periods for the simulation~~
161 ~~experiments,~~ is presented. The ~~parameter calibration and validation of the runoff simulations~~
162 ~~of the forward model and the rainfall simulations of the inverse model is~~ are described in
163 ~~detail~~ in the results and discussion section. ~~Here also different results of the inverse model are~~
164 ~~described and discussed. Apart from results from the calibration and validation period the~~

Formatiert: Englisch (Großbritannien)

Formatiert: Nicht Hervorheben

Formatiert: Nicht Hervorheben

Formatiert: Nicht Hervorheben

Formatiert: Nicht Hervorheben

165 influence of different calibration inputs and system states on the inverse rainfall estimates are
166 presented. Finally the paper ends with a summary and ~~conclusions~~outlook~~conclusions~~.

167 2 Methods

168 2.1 Forward model (Rainfall-runoff model)

169 In the ~~continuous-state space formulated~~ forward model, the unknown runoff Q_t is a function f
170 of known variables rainfall input R_t , potential evapotranspiration ETp_t , system states S_{t-1} and a
171 set of model parameters θ_i , whereas the index t denotes time:

172 $Q_t = f(R_t, ETp_t, S_{t-1} | \theta_i)$ (1)

173 The rainfall-runoff model ~~used~~ is based on the COSERO model (see introduction for
174 references), but has a simpler model structure. It includes an interception and soil module and
175 three reservoirs for interflow, base flow and routing. The model structures is shown in Fig. 1,
176 model parameters are summarized in Table- 2 and fluxes and system states in Table- 3.

- 177
- 178 → Approximate location of Fig. 1
 - 179 → Approximate location of Tab. 2
 - 180 → Approximate location of Tab. 3

181 The COSERO-model is formulated in a state space approach, with state transition functions

182 $S_t = f(S_{t-1}, I_t | \theta_i)$ (2)

183 and output functions

184 $O_t = f(S_{t-1}, I_t | \theta_i)$ (3)

185 with

- 186 I_t Input (~~mm/Δt~~), e.g. rainfall (~~Table- 23~~)
- 187 O_t Output (~~mm/Δt~~), e.g. total runoff (~~Table- 23~~)
- 188 S_t System states (~~mm~~), e.g. water stored in soil module (~~Table- 23~~)
- 189 θ_i Model parameters (Table 2).

Feldfunktion geändert

Formatiert: Englisch (Großbritannien)

Formatiert: Englisch (Großbritannien)

Feldfunktion geändert

These functions have a time component, which is indicated by the index “t”. So, the model state and the output at time t depend only and exclusively on the previous state S_{t-1} , the inputs I_t and parameters θ_i . Schematically the state space approach can be represented as shown in Fig. 2.

→ Approximate location of Fig. 2.

The simplified model formulation can be found in the appendix.

2.2 Inverse model (Runoff-rainfall model)

In the inverse model the unknown rainfall R_t is a function of runoff Q_t , potential evapotranspiration ETp_t , system states S_{t-1} and a given set of model parameters θ_i , whereas where again the index t denotes time:

$$R_t = f^{-1}(Q_t, ETp_t, S_{t-1} | \theta_i) \quad (4)$$

The chief objective in the application of the inverse model is the estimation of rainfall from observed runoff. Given ETp_t , potential evapotranspiration, S_{t-1} , system states and θ_i , model parameters, there is only one single input I_t , which results in an output O_t (eq. (3)). To calculate the inverse rainfall rate the forward model is therefore embedded in a search algorithm, to find, for every time step t, the rainfall rate R_t that best fits the observed runoff. The forward model is embedded in an iteration algorithm, in which for every time step t the rainfall value R_t is determined, which satisfies the function

$$f(R_t) = QSIM_t(R_t, ETp_t, S_{t-1} | \theta_i) - QOBS_t \leq \varepsilon \quad (5)$$

with

$$R_{t,min} \leq R_t < R_{t,max} \quad (6)$$

The upper and lower brackets of rainfall ($R_{t,min}$ and $R_{t,max}$) is set to 0- and 50 mm/h. The value of the upper bound is an reasonable arbitrary value, but any reasonable bounds can be applied. $QSIM_t$ and $QOBS_t$ is the simulated and observed runoff, ε denotes a small value, which is ideally zero. Eq. (5) reflects the objective function used in the search algorithm.

Solving eq. (5), which reflects the objective function used in the search algorithm, is basically a root finding problem. Different root finding algorithms were tested, with the Van Wijngaarden–Dekker–Brent Method (Brent, 1973; Press et al., 1992) being the method of

Formatiert: Englisch (Großbritannien)

Formatiert: Standard, Keine Aufzählungen oder Nummerierungen

Formatiert: Englisch (Großbritannien)

Formatiert: Englisch (Großbritannien)

Formatiert: Tiefgestellt

Formatiert: Tiefgestellt

choice, as this method exhibited the fastest results. The Brent's method combines root bracketing, bisection and inverse quadratic interpolation to converge from the neighbourhood of a zero crossing and will always converge, as long as the function can be evaluated within the initial defined interval (in our case $R_{t,\min}$ and $R_{t,\max}$) known to contain a root (Press et al., 1992). The iteration progress for one model time step is illustrated in Fig. 2. The left y-axis shows the objective function values, the right y-axis (in logarithmic scale) the associated rainfall values estimated during the iteration procedure.

➔ Approximate location of Fig. 2

~~In every time step the forward model is applied, resulting in an inverse rainfall value and the corresponding runoff and system states.~~ The state space approach of the model is a first order Markov process: The system states S_t and outputs O_t of the calculation time step depend only on the preceding states S_{t-1} and some inputs I_t and not on the sequences of system states, that preceded it, e.g. S_{t-2} , S_{t-3} , ..., S_{t-n} (see eq. (2) and eq. (3)). All information of the sequence of the preceding inputs (I_{t-1} , I_{t-2} , ..., I_{t-n}) is implicitly included in the last relevant system state S_{t-1} . No hysteretic effects are considered in the model and it does not include a parameter, which introduces a lag effect between inputs and outputs.

~~Given the model structure, parameters and potential evapotranspiration as input, the inverse rainfall and resulting runoff are solely a function of the initial cold system states. The influence of the initial cold system states on the inverse rainfall calculation Section 4.3.4 of this paper is analysed in the results section. committed to analysing the influence of the initial cold system states on the inverse rainfall calculation.~~

The determined rainfall value R_t represents the “best” simulated rainfall of the catchment and ~~can is~~ also ~~be~~ used as input into the forward model to simulate runoff. Therefore, for every time step the inverse model simulates a rainfall and ~~a~~ corresponding runoff value ~~and also resulting system states~~. The simulated runoff value should ideally be identical to the observed value. This is however not always the case, as will be shown later.

A more elegant method to calculate rainfall from runoff ~~is~~ by analytically inverting the ~~model~~ equations ~~of a given model, i.e. bringing the rainfall term onto the right side of the equation (Herrnegger, 2013). This~~ is principally possible, but has some disadvantages ~~(Herrnegger, 2013). The model structure, which was used in Herrnegger (2013) and which can be inverted~~

analytically, differs from the model presented here. It does not include interception and routing. Additionally the inversion is not possible in certain periods, since the discontinuities introduced by threshold values lead to non-inversibility in the analytical solution (Herrnegger, 2013). For the forward model used here, the differential equations of the linear reservoirs are solved analytically. An internal time step discretization is included in the model code to guarantee, that the transition between system states above and below the threshold value are solved exactly. This is not possible in the analytical solution.

Solving eq. (5) is basically a root finding problem. Different root finding algorithms were therefore tested, with the Van Wijngaarden-Dekker-Brent Method (Brent, 1973; Press et al., 1992) being the method of choice, as this method exhibited the fastest and most robust results. The Brent's method combines root bracketing, bisection and inverse quadratic interpolation to converge from the neighbourhood of a zero crossing and will always converge, as long as the function can be evaluated within the initial defined interval (in our case $R_{t,min}$ and $R_{t,max}$) known to contain a root (Press et al., 1992). The iteration progress for one model time step is illustrated in Fig. 3. The left y axis shows the objective function values, the right y axis (in logarithmic scale) the associated rainfall values estimated during the iteration procedure.

→ Approximate location of Fig. 3

2.2.1 Preconditions and Limitations of the application of the inverse model

It ~~is~~ must be assumed that ~~all~~ runoff from the catchment passes through the measurement ~~cross-cross~~ section of the gauging ~~station-station~~ and that ~~S~~ subsurface and transboundary flows are ~~assumed to be~~ negligible. It does not make sense to apply the inverse model to leaky catchments or catchments, where a significant part of the runoff is not observed at the gauging site. Even with a given quantification of the leakage process, the application of a hydrological model would lead to an additional uncertainty difficult to quantify. This is however not necessarily a limitation of the inverse model. Also the application of a forward hydrological model, which needs to be calibrated against runoff observations, will fail or will result in wrong estimates of water balance components.

The inverse model is based on a lumped model setup. ~~Therefore and~~ the resulting inverse rainfall value corresponds to the mean areal rainfall. Applying a spatially distributed model is not possible, since the origin of outputs of different zones or cells of a distributed model setup cannot be reproduced by the inverse model in a deterministic way without additional

~~assumptions without additional information~~. The information of origin gets lost as soon as cell values are summed and routed to a catchment runoff value. It is however conceivable to spatially disaggregate the mean areal rainfall from the inverse model using additional information, e.g. assuming an elevation dependency of rainfall.

~~Solid rainfall~~precipitation is accumulated without any direct signal on the hydrograph. It is therefore impossible to use the inverse model to estimate solid precipitation~~rainfall~~. The inverse model can therefore only be used to calculate rainfall in snow-free catchments, or, as in our case, periods, in which runoff is not influenced by snow melt (i.e. summer months). However, in rainless periods, where it is clear, that snow melt is dominating runoff (e.g. in spring), the inverse model can be used to quantify the snow melt-contribution rates from a catchment.

The applicability of the inverse model is limited to catchments, which are representable with a lumped model setup and the proposed model structure. If a catchment is too large, one will generally have problems modelling that system with a lumped model setup. Not necessarily because of neglecting spatial heterogeneity in the model parameters (although this is may also be an issue) or ignoring a lag between the rainfall and runoff signal, but simply because the lumped rainfall input used is “wrong” and is not representable for the whole catchment. If it only rains in the headwaters of large catchment, the lumped input into the forward model for this time step or rainfall event will be much lower, since it will be spatially aggregated. This input is simply not applicable to the whole catchment and the simulations will show deficits. In this case, an inversion also does not make senseinversion will be highly flawed.

It is also evidentclear, that catchments, independent of size, exist, where the application of this particular model structure will fail (e.g. flatland catchments dominated by groundwater). If hydro-meteorological conditions of the catchment change or are different from the calibration period and the forward model (e.g. due to poor parameter estimation, inadequate model structure, wrong representation of the real world prototype etc.) is not able to capture these changes, then again the calculation of rainfall from runoff will fail (as they do for the forward case).

However, being able to fitwhen you are able to fit the forward model to observed runoff data and as long as the forward model is able to represent the catchment responses to rainfall, an inversion will be possible.

~~The inverse model can only be applied in snow free catchments or periods without snow. Snow models accumulate snow in a “reservoir without memory”, as solid Solid rainfall is accumulated without the information of point in time any direct signal on the hydrograph. It is therefore impossible to invert snow models use the inverse model to estimate solid rainfall. The inverse model can therefore only be used to calculate rainfall in snow free catchments, or, as in our case presented in this paper, periods, in which runoff is not influenced by snow melt (i.e. summer months). However, in rainless periods, where it is clear, that snow melt is dominating runoff (e.g. in spring), the inverse model can be used to quantify the snow melt contribution.~~

2.3 Simulation setups

2.3.1 Virtual experiments

~~In a first step the inverse model is evaluated and tested with virtual experiments, in which the preconditions of existence, uniqueness and stability of the inverse rainfall values are evaluated, with virtual experiments. Very small errors resulting from numerical issues in single modules, e.g. the soil layer, propagate through the model cascade and can be amplified, leading to erroneous results. As the model is formulated in a state space approach, outputs are also dependent on the system states of a given time step. It is therefore quite conceivable, that a combination of different system states can lead to identical realisation of rainfall results. Finally, an inverse rainfall value calculated in one time step directly influences the system states for the next time step. Erroneous inverse rainfall values can therefore lead to unstable results. For the virtual experiments, runoff Runoff simulations are performed with the forward models driven with by observed rainfall as input. The simulated runoff time series of the forward models are then used as input into the inverse model, with the aim to reproduce the observed rainfall originally used as driving input in the forward model. Simulated runoff from the forward model is dependent on the model parameters. Therefore, to test the inversion procedure for the whole parameter range, synthetic hydrographs are produced with Monte Carlo simulations. 20 000 different parameter combinations are chosen randomly from the parameter space, with the same number of model runs to evaluate the inverse model. The sampled parameters and associated range is are shown in Table 2. The schematic setup of the virtual experiment and the evaluation of the inverse model is shown in Fig. 43. Note, that the~~

Formatiert: Überschrift 2

setup and the evaluation is performed for every individual Monte Carlo run, as the simulated runoff from the forward model varies, depending on selected model parameters.

→ Approximate location of Fig. 43

The virtual experiments enable a rigorous evaluation of the inverse calculations, neglecting uncertainties concerning measurement errors in runoff, model structure or model parameters.

All system states, ~~variables~~ and fluxes of the forward model are perfectly known at every ~~point in time~~ time step. This information is used to evaluate the inverse models. Only after a successful evaluation of the inverse model with the virtual experiments, can observations of runoff be used as input into the inverse models.

2.42.3.2 Model calibration and simulations experiments with observed ~~rainfall as input data~~

~~The application of the inverse model is based on the assumption that the forward model is able in representing~~ can represent the catchment responses to rainfall, but needs to be calibrated against runoff observations. Depending on the calibration setup, different model parameters will be estimated. The calibration setup and in consequence model parameters (for a given model structure) can depend on (i) the calibration period and length and (ii) the driving input used. The inverse rainfall is also a function of the observed runoff, which may also exhibit possible measurement errors. Finally, the initial conditions of the system states at the beginning of the simulations also influence the results of the forward, but also inverse model. To evaluate these influences, i.e. different model parameters due to different calibration periods and lengths, different runoff observations, different parameter optimisation data basis and different initial conditions, several simulation experiments are performed. An overview table of the simulation experiments can be found in section 3.3 (Table 5) after the presentation of the available data.

~~The model structure applied includes 12 parameters, of which 10 have to be calibrated. 2 Two P~~parameters (INTMAX and ETVEGCOR) are estimated a priori (see Table 2). The simulation experiments do not allow a systematic analysis of parameter uncertainty or the assessment of equifinality. This is not the aim of this paper. The simulation experiments however enable a first assessment of the robustness of the results. That is to show the forward and inverse model performance, when the conditions are different from the conditions the model has been calibrated against or if different driving inputs are used ~~for calibration~~.

Formatiert: Überschrift 3

In a first step 3 different periods are used for calibration of the model parameters. In a further simulation experiment, the runoff observation is increased by a constant offset of 10% to evaluate the influence of possible streamflow errors on the simulations and the inverse rainfall. A fifth experiment is performed, in which a differing rainfall realisation is used as driving input for model calibration, in order to test the conditioning of the model parameters and in consequence the simulations to the driving input. Given the model structure, the inverse rainfall is a function of observed runoff, potential evapotranspiration, system states and model parameters (see eq. (4)). Extending eq. (4) explicitly with all relevant system states (see Table 3) leads to

$$R_t = f^{-1}(Q_t, ETp_t, BWI_{t-1}, BW1_{t-1}, BW2_{t-1}, BW3_{t-1}, BW4_{t-1} | \theta_i) \quad (7)$$

The forward and inverse models are run as a continuous simulation in time (Fig. 2). The preceding system states are therefore an integral part of the simulation and are determined intrinsically within the simulation. However, the initial system states at the beginning of the simulation period (cold states) will influence the results of the simulation, but should, after an adequate spin-up time, not influence the runoff but also inverse rainfall estimates. To evaluate the influence of cold states on the inverse rainfall, therefore, a sixth experiment was set up, in which 3 different cold start scenarios are defined:

- Reference scenario
- Dry system states scenario
- Wet system states scenario

For the reference scenario the system states from the continuous simulation were used. For the cold states in the dry scenario the states from the reference scenario were reduced by the factor 0.5 and increased by the factor 1.5 for the wet scenario.

Generally only June, July, August and September are used, since it can be guaranteed, that no snow melt influences runoff in these months (see section 2.2.1). Parameter calibration in the simulation experiments is performed for the forward model, using the Shuffled Complex Evolution Algorithm (Duan et al., 1992) to automatically optimise model parameters. As an optimisation criterion the widely used Nash-Sutcliffe-Efficiency (NSE, Nash and Sutcliffe, 1970) was chosen. The optimised parameters are used in the inverse model to calculate rainfall from observed runoff (Fig. 5).

Formatiert: Englisch (Großbritannien)

Formatiert: Englisch (Großbritannien)

Formatiert: Aufgezählt + Ebene: 1 + Ausgerichtet an: 0.63 cm + Einzug bei: 1.27 cm

→ Approximate location of Fig. 5

~~To evaluate the influence of model parameters on the simulated runoff and inverse rainfall, different simulation experiments are performed. 2 different data sets of observed rainfall are used as calibration input in the forward model, resulting in 2 different parameters sets for simulating inverse rainfall. Model parameters are also evaluated in independent validation periods.~~

3 Materials

3.1 Study areas

The inverse model is applied to two catchments with different size, geology and land use located at the foothills of the Northern Alps. The Schliefau catchment is located about 110 km south-west of the Austrian capital of Vienna and covers an area of 17.9 km² with a mean elevation of 608 m.a.s.l.. About 55% of the area is covered by grassland and meadows, 40% by coniferous forest and 5% by mixed forest. The underlying geology is dominated by marl and sandstone. The Krems catchment is located about 170 km south-west of the Austrian capital of Vienna and covers an area of 38.4 km² with a mean elevation of 598 m.a.s.l.. The topography is more heterogeneous, with an elevation range of 413 to 1511 m.a.s.l., compared to 390 to 818 m.a.s.l. in the Schliefau catchment. Approximately 46% of the area is covered by grassland and meadows, 48 % by mixed forest, 4 % by settlements and 2 % by coniferous forest. On a long term basis, in both catchments, ~~In both catchments and on a long term basis t~~ the highest runoff can be expected during snow melt in spring, the lowest runoff in summer and autumn until October. Fig. ~~6-54~~ shows a map of the catchments and ~~Tab~~e 4 summarizes ~~some-important~~ characteristics of the study areas, ~~which also shows, that the Krems catchment is wetter, compared to the Schliefau watershed.~~

→ Approximate location of Fig. 4

→ Approximate location of Tab. 4

→

3.2 Meteorological database

Generally, two different rainfall time series are used. Ground observations of rainfall are available from the station St. Leonhard im Walde (Schliefau catchment) and Kirchdorf

(Krems catchment), both located in the proximity of the catchments (Fig. 654). ~~For additional evaluation of the rainfall calculated by the inverse model.~~ Additionally, areal rainfall data from the INCA system (Integrated Nowcasting through Comprehensive Analysis; Haiden et al., 2011) is used. INCA is the operational nowcasting and analysis application developed and run by the Central Institute for Meteorology and Geodynamics of Austria (ZAMG), which is also used for the majority of real-time flood forecasting systems in Austria (Stanzel et al., 2008). For the presented study analysis fields derived from observations, but no nowcasting fields, are used. Rainfall in INCA is determined by a nonlinear spatial interpolation of rain-gauge values, in which the radar field is used as a spatial structure function. In addition an elevation correction is applied (Haiden and Pistotnik, 2009). The stations used for the interpolation of the INCA-rainfall fields are shown as triangles in Fig. 654. Note, that the stations St. Leonhard im Walde and Kirchdorf are not included in the INCA analysis, ~~since they are operated by a different institution.~~ The rainfall fields from the INCA system cover the test basins in a spatial resolution of 1 km². From the spatial data set mean catchment rainfall values are obtained by calculating area-weighted means from the intersecting grid cells.

Potential evapotranspiration input is calculated with ~~the a~~ temperature and potential radiation method ~~of Hargreaves~~ (Hargreaves and Samani, 1982).

➔ ~~Approximate location of Fig. 65~~

3.3 Simulation periods

~~Runoff and rainfall data is available for the period 2006 to 2009 in a temporal resolution of 60 minutes, which is also the All simulations are performed with a temporal resolution of 60 minutes-modelling time step.~~ The virtual experiments are performed for a period of 4.5 months (15.5.2006 – 30.09.2006) resulting in 3336 time steps being evaluated. ~~Calibration of the model parameters is carried out for the years 2006 to 2008. Data from the year 2009 is used for validation purposes.~~ As described in section 2.3.2 different model calibration and simulation experiments are performed. An overview of these experiments is given in Table 5.

➔ ~~Approximate location of Tab.5 Note, that Only the snow-free months of June, July, August and September are evaluated, as only in these months it can be guaranteed, that no snow melt contribution influences runoff. Rainfall time series for calibration~~

Formatiert: Listenabsatz, Aufgezählt + Ebene: 1 + Ausgerichtet an: 0.63 cm + Einzug bei: 1.27 cm

and validation from the station Kirchdorf are used. Additional tests of the inverse model are performed using the INCA data as calibration input.

4 Results and discussions

4.1 Virtual experiments

In the virtual experiments it could be ~~proven~~shown, that the precondition of existence, uniqueness and stability of the inverse model results is given. Using all ~~20-20~~ 000 simulated hydrographs from the Monte Carlo runs, where the parameters were varied stochastically, the observed rainfall time series could be identically reproduced by the inverse model. Apart from the rainfall also all fluxes and system states ~~and model variables~~ where identical in the forward and inverse model runs. The comprehensive R_e results from the virtual experiments are documented in Herrnegger (2013). Fig. 65 shows as an example of the virtual experiments the identical (i) observed rainfall POBS and simulated inverse rainfall and (ii) system state of soil water content from the forward and inverse model. The station data from the Schlieffau catchment using with model parameters of Exp3 (see Table 5) was used as driving input in the forward model and the resulting runoff simulation in succession as input into the inverse model.

→ Approximate location of Fig.65

4.2 Forward model: Parameter calibration and validation of the different simulation experiments of the forward model

A precondition for the application of the inverse model is that the observed runoff characteristics of the catchment are reproduced reasonably by the forward model, since these parameters are also used in the inverse model. The following section therefore ~~shortly~~ presents the runoff simulations of the forward model, based ~~on the model parameters optimised with the rainfall time series of the station Kirchdorf as input~~ on the different simulation experiments Exp1 to Exp5.

The model performance for the ~~calibration period~~ period 2006 to 2009 of the forward model, expressed by Nash-Sutcliffe-Efficiency (NSE) ~~Pearson's correlation (CORR)~~ and the mean bias between simulated and observed runoff in percent of observed runoff ~~Nash-Sutcliffe-~~

Formatiert: Mit Gliederung + Ebene: 2 + Nummerierungsformatvorlage: 1, 2, 3, ... + Beginnen bei: 1 + Ausrichtung: Links + Ausgerichtet an: 0 cm + Tabstopp nach: 1.02 cm + Einzug bei: 1.02 cm

Formatiert: Listenabsatz, Aufgezählt + Ebene: 1 + Ausgerichtet an: 0.63 cm + Einzug bei: 1.27 cm

Formatiert: Mit Gliederung + Ebene: 2 + Nummerierungsformatvorlage: 1, 2, 3, ... + Beginnen bei: 1 + Ausrichtung: Links + Ausgerichtet an: 0 cm + Tabstopp nach: 1.02 cm + Einzug bei: 1.02 cm

Efficiency (NSE), is shown in Fig. 76. As mentioned before, only the months June, July, August and September of the single years are used.

Approximate location of Fig. 76



For Exp1 to Exp3, the NSE-values of Exp1 to Exp3 for the period 2006 to 2009 show, that the overall model performance is fairly stable and comparable, independent of the calibration length. The NSE-values are larger than 0.82, with the exception of Exp1 in the Krems catchment. It is noteworthy, that although the calibration lengths and periods in Exp2 and Exp3 differ, identical model parameters were found for the Krems catchment in the optimisation for both simulation experiments. As a consequence the model performance is identical between these two experiments for the period 2006 to 2009. The mean bias does not show a clear pattern and seems to be independent from the calibration period and length. In the Schlieffau catchment observed runoff is overestimated by 7.8 to 0.9 % and underestimated by -1.4 to -4.8% in the Krems catchment for the period 2006-2009, depending on the simulation Exp1 to Exp3. Overall the calculated bias between observed and simulated runoff is in reasonable bounds.

In Exp4 the observed runoff is increased by 10%, mainly to evaluate the influence of possible streamflow errors on the simulations and the inverse rainfall. The same calibration and validation periods were used as in Exp3, with station observations as driving input into the model. Concerning the NSE, the model performance NSE of Exp4 is comparable to Exp1, Exp2 and Exp3. The model parameters compensate the bias introduced due to the increase of observed runoff. The mean bias in Exp4 however becomes negative larger, since the observed runoff is now also underestimated in the Schlieffau catchment, what is not surprising, since observed runoff was increased. The mean bias in Exp4 for the Krems catchment is also larger, compared to Exp1 to Exp3. This is also explained by the increased observed runoff.

In Exp5 INCA rainfall data is used as driving input for the simulations. The main intention of Exp5 is to evaluate the influence of a different rainfall input on the calibration of the model parameters and in consequence also on the inverse rainfall. For both catchments, the NSE values of the forward model are significantly lower, also compared to Exp3, which has the same calibration and validation periods. Although INCA uses a complex interpolation

scheme, also incorporating radar data (Haiden et al., 2011), it seems that the data set has deficits representing catchment rainfall compared to the station observations in the proximity of the catchments. This can be explained by the larger distance of about 10 to 35 km of the INCA stations from the catchment (see Fig. 54) and highlights the importance of ground observations. Note, that the ground observations in the proximity of the catchments are not used in the interpolation process for the INCA-rainfall fields, as they belong to a monitoring network operated by a different institution.

Fig. 76 shows the NSE-values of the forward model for the calibration periods of every simulation experiment versus single years performance for the 2 study areas.

→ Approximate location of Fig.76

→ Especially for Exp1 a significant larger spread in the model performance within the single years is evident. In Exp1 only 2006 was used for calibration. As a consequence, especially for the Krems catchment, the model performance is significantly lower in the years 2007 to 2009, compared to Exp2 and Exp3. In the short calibration period of 2006 the model parameters are overfitted to the observations. If the conditions in the catchment are different from the calibration period, the model performance can be expected to deteriorate, as has been shown before. This has been shown before (e.g. Kling, 2015; Seibert, 2003) and explains the findings. For Exp2 to Exp4 the model performance is however stable for the single years, also for 2009, which was not used for calibration in any simulation experiment. In contrary to the Krems area, a large spread in the model performance of the single years for Exp5 is visible in the Schlieffau catchment. The reason is not clear and may be explained by changing availability of station data for the INCA rainfall in the single years. We can however not verify this hypothesis, since we do not have access to the data sets. In the Schlieffau catchment low NSE values are calculated for the year 2008 for all simulation experiments. In the beginning of June a flood was observed (see Fig. 87), which is not simulated in the model runs and explains the lower NSE values in this year. Excluding this event in the performance calculations would, for example, result in a significantly higher NSE of 0.84 for Exp1 for the year 2008, compared to 0.63 when the flood event is included in the calculation.

Formatiert: Standard, Keine Aufzählungen oder Nummerierungen

~~The correlation between simulated and observed runoff in different years lies between 0.89 and 0.95. The NSE values range from 0.78 and 0.89. Evaluating all relevant months (June, July, August and September) for the period 2006-2008 yields an overall correlation of 0.92 and a NSE value of 0.84. It can be concluded that the model performance within the years is fairly stable and comparable.~~

~~Fig. 778 (Schliefau) and Fig. 898 (Krems) exemplarily show the runoff simulations based on the results of Exp2 as an example. This simulation experiment was chosen for no specific reason. Generally~~For both catchments, the dynamics and variability of the runoff observations are mostly reproduced in a satisfactory ~~manor~~manner. However, a tendency is visible, that larger floods are underestimated in the simulations, by the forward model (Fig. 8). Although there is a tendency of underestimating runoff observations as indicated by the regression line, no obvious systematic errors are visible from the scatter plot (Fig. 9).

→ Approximate location of Fig. ~~787~~

→ Approximate location of Fig. ~~988~~

~~The validation of the forward model yields good results. In the year of 2009 a NSE of 0.86 and a correlation value of 0.93 is obtained. Thus, the model efficiency is comparable to the calibration period.~~

~~The~~All simulations are performed with a lumped model setup. Consequently heterogeneity in geology and land use within the catchment are not ~~explicitly~~ considered in the parameter estimation. Also Taking this into consideration, it can be concluded that the general responses of the catchment to rainfall input are captured appropriately by the forward model. Only for Exp1 with the very short calibration period, a larger spread in the model performance is evident in independent years. This is the case for the presented simulation experiments. It is therefore justified to calculate areal rainfall from runoff using the inverted forward model, including the optimised parameters.

4.3 Inverse model

For the evaluation of the simulated rainfall from the inverse model (PInv) we will compare the calculated values with observed station data (POBSbs) of St. Leonhard (Schliefau catchment) and Kirchdorf (Krems catchment) and the rainfall values from the INCA-system

Formatiert: Standard, Keine Aufzählungen oder Nummerierungen

(PInca). In the following cumulative rainfall sums and the correlation and bias between simulated and observed rainfall are presented. Additionally the rainfall and runoff simulations of a flood event and the influence of cold system states on the simulations are shown. The ground observations are not used in the interpolation process for the INCA rainfall fields, as they belong to a monitoring network operated by a different institution (see Fig. 5). Generally, the inverse rainfall results are presented with cumulative rainfall diagrams, scatterplots, time series plots and different objective performance criteria.

4.1

4.1.4.3.1 Calibration period Cumulative rainfall sums

For the evaluation of the simulated rainfall from the inverse model (Inverse P) we will compare the calculated values with observed data of the Kirchdorf station (POBS) and the rainfall values from the INCA system (INCA). The ground observation is not used in the interpolation process for the INCA rainfall fields, as it belongs to a monitoring network operated by a different institution (see Fig. 6). Generally the inverse rainfall results are presented with cumulative rainfall diagrams, scatterplots, time series plots and different objective performance criteria.

Fig. 9+10 and 11 show the cumulative curves of the observed rainfall (POBS), INCA rainfall (PInca) and the inverse rainfall (PInv) of the simulation experiments Exp1 to Exp5 for the Schliefaue and Krems catchment. Additionally the cumulative observed runoff (Qobs) is shown as a dashed line. Note that for the Krems catchment (Fig. 10+11) the rainfall curves of Exp2 and Exp3 are identical, since the model parameters are also identical in these simulation experiments.

→ Approximate location of Fig.9

→ Approximate location of Fig.10

The cumulative sums of the inverse rainfall and the observation based rainfall realisations POBS and PInca mostly show very similar temporal dynamics. Although large deviations are sometimes evident for both catchments, the deviations of the cumulative curves of PInca and the different inverse rainfalls (PInv) from the cumulative curves of the ground observation (POBS) are mostly of similar magnitude. At the beginning of June 2008 a flood

Formatiert: Standard

was observed in the Schlieffau catchment, which was underestimated in the forward simulation (see runoff simulation in Fig. 78, lower left). Larger rainfall intensities are therefore calculated by the inverse for this period, leading to the larger deviations between the cumulative sums of POBS and PInv of Exp1 to Exp5 as shown in Fig. 910 (lower left).

Generally, the inverse rainfall curves of Exp1 to Exp5 of the two catchments are mostly very similar and do not exhibit substantial differences, although different calibration periods and setups were used. At the beginning of June 2008 a flood was observed in the Schlieffau catchment, which was underestimated in the forward simulation, presumably due to inadequate representation of the storm event in the rainfall observations (see runoff simulation in Fig. 7, lower left). Larger rainfall intensities are therefore calculated by the inverse for this period, leading to the larger deviations between the cumulative sums of PObs and PInv of Exp1 to Exp5 as shown in Fig. 9 (lower left). In the Schlieffau catchments larger differences between Exp1 to Exp5 occur in the year 2009 (Fig. 9, lower left/right). Here, in the second half of June, a period of strong rainfall is evident, which also led to a series of floods in the catchment (see also the hydrographs in Fig. 787). The rainfall sums originating from these high flows were calculated differently in the inverse models, depending on the simulation experiment. In consequence, the inverse rainfall curves differ from July onwards. In 2009, which was the wettest summer in both catchments, the highest inverse rainfall sums are found for Exp4. This is what could be expected, since the observed runoff was increased by 10% in this simulation experiment. However, in the other years Exp4 does not necessarily show the largest inverse rainfall sums. The optimised model parameters in Exp4, that control evapotranspiration, were limiting actual evapotranspiration from the model to fulfil the water balance, since POBSbs was not changed. In the second half of June 2009, during the flood events with low evapotranspiration, the higher runoff values used as input however show a clearer signal in the inverse rainfall sums.

different rainfall realisations (Fig. 10) show very similar temporal dynamics. Although large deviations are sometimes evident, the deviations of the cumulative curves of INCA and inverse rainfall (Inverse P) from the cumulative curves of the ground observation (POBS) are generally of similar magnitude. For the months June and July in 2006 the cumulative sum of the inverse rainfall for example follows POBS more closely compared to the INCA data set. Around the 01.08.2006 a period of higher runoff was observed in the catchment (Fig. 8). During this event the higher rainfall compared to POBS was simulated by the inverse model,

explaining the stronger increase in the inverse rainfall sum during this period. As a results the inverse rainfall sum converges towards the INCA data.

— Approximate location of Fig.109

→ Approximate location of Fig.110

For the period in 2007 the cumulative inverse rainfall sums agree very well with the curve of POBS. In this year the deviations of the INCA data from POBS are higher. In the period of 2008 the deviation of the inverse rainfall sums from POBS data are slightly higher compared to INCA data. The large difference between comparison of the cumulative rainfall and runoff curves in Fig. 9 and 10 highlight the importance of actual evapotranspiration (AETa) in the catchments. For the Schlieffau catchment the mean observed rainfall for the summer months of 2006-2009 is 678 mm. 266 mm are observed in the mean for runoff. Neglecting storage effects, a mean actual evapotranspiration of 412 mm can be calculated from the water balance. Over 60 % of rainfall are therefore lost to evapotranspiration. The mean actual evapotranspiration from the inverse model, depending on the simulation experiment, range from 352 mm to 362 mm, and are lower compared to the AETa calculated from the water balance. In the Krems catchment a mean runoff of 334 mm and rainfall of 600 mm, resulting in an actual evapotranspiration of 266 mm, is calculated. Although lower compared to Schlieffau, nearly 45 % of rainfall are here lost to the atmosphere. The mean actual evapotranspiration from the inverse model, again depending on the simulation experiment, range from 276 mm to 310 mm, with Exp4 showing the highest value. ETa AET from the model reflects the complex interplay and temporal dynamics of the system states of the different parts of the model. If the model would not capture ETa AET adequately, the cumulative rainfall curves would not follow the observations so closely.

On the basis of the different cumulative rainfall sums it can therefore be concluded, that on a longer temporal basis, the inverse model is capable of simulating the catchment rainfall from runoff observations. The results from the different simulation experiments do not differ substantially and show close correspondence to the observed data, not differing substantially, except for a single summer in the Schlieffau catchment.

4.3.2 Correlation and bias between simulated and observed rainfall

The scatterplots in Fig. 11 show the relationships between the different rainfall realisations for 1 h, and aggregated 6 h and 24 h rainfall sums. Note, that the hourly data corresponds to the

Formatiert: Überschrift 3

modelling time step. The relationships between ground observation and inverse rainfall (POBS – Inverse P) are shown in Fig. 11 (a) – (e)). In the second row ground observation versus INCA rainfall (POBS – INCA; Fig. 11 (d) – (f)) are shown.

→ Approximate location of Fig.11

It can be summarised:

— In the POBS – Inverse P case (Fig. 11 (a) – (e)) the monitored rainfall data are in many cases lower, especially for 1 h sums. For some observed high rainfall intensities, the inverse model yields no or very low rainfall intensities. This occurs in periods, in which simulated runoff from the inverse model is larger than observed runoff, as no rainfall is estimated in the inverse model.

— In the POBS – INCA case (Fig. 11 (d) – (f)) the INCA data yields lower values than observations, especially for higher intensities in the 1 hour sums, but also for longer time intervals. The INCA interpolation method obviously smoothes the rainfall field with a high temporal resolution. It is noticeable, that for some point observations with no or little rainfall, INCA predicts rainfall. This is explained by the relative large mean distance between the stations used for the INCA interpolation and the catchment, which is about 17 km.

— Especially for the hourly data a large scatter around the 1:1 line is found for both cases, also explaining the low coefficient of determination (R^2) values.

— Generally, for longer time intervals $\Delta t \geq 6$ h all datasets are in good agreement.

Compared to INCA, the coefficient of determination (R^2) between observed data and inverse rainfall is slightly higher ($R^2=0.24$ vs. $R^2=0.18$, Fig. 11 (a), (d)). For the 6 h and 24 h sums similar coefficients of determination, which are considerably higher compared to the 1 h sums, are calculated (Fig. 11 (b) and (e); Fig. 11 (e) and (f)).

The model performance of the inverse model expressed by the correlation coefficient is used to measure the models ability to reproduce timing and shape of observed rainfall values. It is independent of a possible quantitative bias. In the introduction the difficulties involved in the quantitative measurement of rainfall were discussed. It can, however, be assumed that a qualitative measurement, e.g. if it rains or not, will be more reliable. FigTable- 127 shows the correlation values for 2006 to 2009 between ground observation observations and the different inverse rainfall realisations (POBS-PObs – Inverse-PPInv) and ground observations and INCA rainfall (POBS-PObs – INCA-PIInca) for different periods and temporal aggregation lengths.

→ Approximate location of [FigTab.127](#)

~~For the 1h-sums, the lowest correlation values between PObs and PInv are found for the simulation results of Exp1 in both catchments and all aggregation lengths. For the 1h-sums~~
~~the~~ The highest correlation values are found for Exp2 in the Schliefauf catchment and Exp2 to Exp4 in the Krems catchment. This also agrees with the findings performance of the forward model presented in section 4.2. ~~from the runoff simulations.~~ The correlation of the 1h-sums between PObs and PInv is rather weak. However, ~~the~~ the correlation between PObs and PInv is higher ~~or of the same magnitude~~ for all simulation experiments and 1h-sums compared to the correlation between PObs and PInca. This is interesting, since PInca is based on station rainfall observations and PInv is indirectly derived from runoff through simulations. With temporal aggregation the correlation values generally increase significantly for all combinations. Small differences or timing errors in the 1h-sums are eliminated with temporal aggregation. This is also the case in of the INCA data.

For Exp1 to Exp4, the model parameters used for the forward and inverse model were automatically calibrated using the ground observation PObs as input. It could therefore be concluded that the model parameters are conditioned by PObs and that in consequence the fairly good agreement between PObs and PInv originates from this conditioning. Based on this hypothesis, calibrating the model with INCA data should lead to a better agreement between the INCA data and the corresponding inverse rainfall and a deterioration of the correlation between station data and inverse rainfall. For Exp5, the forward model was therefore calibrated with INCA data and the resulting parameters set was then used to calculate the inverse rainfall. The correlation between PInca and PInv for Exp5 is however not higher, compared to the other simulation experiments and Exp3, which had the same calibration period. This excludes that the parameters are conditioned (at least for the rainfall simulations) by the input used for calibration. The correlations between PInca and PInv are generally very weak, with values ranging from 0.25 to 0.29 for the Schliefauf and 0.39 to 0.445 for the Krems catchment. This corresponds to the performance of the forward model in Exp5. Here lower model performance of the forward model is found for the Schliefauf catchment.

The correlation between PObs and PInv for the 1-h sums ranges between 0.48 and 0.55, but is higher, compared to the correlation between PObs and PInca. In contrast Kirchner (2009) shows correlation values between simulated and observed rainfall of 0.81 and 0.88 for his two

~~sites and presumably on the basis of 5 years of data.~~ The Schlieffau and Krems catchments differ substantially in size, hydrological characteristics, land use or geology. The NSE values of the runoff simulations in Kirchner (2009) are higher, compared to the values presented here for the forward model. As a consequence the better performance in the rainfall simulations may be explained with the fact, that the Kirchner (2009) model better reflects the catchment conditions leading to runoff.

For the 24-h sums we calculate a correlation of 0.87 to 0.92, depending on the catchment and simulation experiment. Here Kirchner (2009) shows correlation of 0.96 and 0.97. Krier et al. (2012) present correlations between simulated and observed rainfall of 0.81 to 0.98, with a mean value of 0.91 for a total of 24 catchments, however only on the basis of data of a single year. The correlation in our results is therefore in the range of other studies. Unfortunately Krier et al. (2012) do not present NSE values of the runoff simulations. It is therefore not possible to check the link between the performance of the forward model and rainfall simulations in their study.

Fig. 11 shows the correlation between PObs and PInv for the calibration periods of the simulation experiments Exp1 to Exp5 versus the correlation in single years for the two study areas. For the Schlieffau catchment the largest spread in the correlation values of the single years is found for Exp1, which also corresponds to the performance of the runoff simulations of the forward model. For Exp2 to Exp5 a spread is also visible between the single years, but differences are smaller. For the years 2006, 2008 and 2009 the correlation values in the Krems catchment do not differ substantially. Here however the correlation for the year 2007 is very low, independent of the simulation experiment. This may be explained by the comparatively dry summer of 2007. Also in the Schlieffau catchment the correlation values are mostly lower in 2007, compared to the other years.

➔ Approximate location of Fig.11

Tab. 8 summarizes the mean daily bias in mmd^{-1} for the summer months in 2006 to 2009 between different rainfall realisations. For the Schlieffau catchment, the bias between PInv and PObs is mostly significantly higher, compared to the bias between PInca and PObs. Only Exp2, with a mean bias of 0.07 mmd^{-1} , is comparable to the bias between PInca and PObs of 0.02 mmd^{-1} . Exp2 also showed the highest performance in the runoff simulations concerning the NSE. In contrary, for the Krems catchment, the bias is lower between PInv and PObs for Exp1 to Exp3, compared to PInca-PObs. For Exp1 to Exp3 a mean bias of 0.14 mmd^{-1}

(Schliefau) and 0.36 mmd^{-1} (Krems) is calculated. As a comparison, Krier et al. (2014) published mean bias values between simulated and observed rainfall of -3.3 to 1.5 mmd^{-1} (mean -0.35 mmd^{-1}) for 24 catchments on the basis of a single year. From all simulation experiments, Exp4 shows the largest bias, which is explained by the fact, that runoff was increased in this experiment. Here the increased runoff clearly shows a signal in the inverse rainfall, in contrast to the correlation and cumulative sums shown above.

→ Approximate location of Tab.8

~~which showed, that for the period 2006-2009, Exp2 performed best in the Schliefau area. In the Krems catchment Exp4 performed best. Generally, the correlation values between ground observations and inverse rainfall and INCA increase with temporal aggregation levels/lengths. The correlation between ground observations and inverse rainfall is higher or of the same magnitude compared to the correlation between ground observation and INCA rainfall. An exception is seen here for the year 2007, where the correlation between POBS and inverse P is considerably lower compared to POBS and INCA.~~

~~Fig. 13 shows the mean squared error (MSE) between ground observation and INCA (POBS — INCA) and ground observation and inverse rainfall (POBS — Inverse P) for temporal aggregation lengths of 1 hour (Fig. 13 (a)), 6 hours (Fig. 13 (b)) and 24 hours (Fig. 13 (c)). With ground observations as a basis, the evaluation with the correlation coefficient suggests that the quality of the temporal dynamics of the rainfall values from the inverse model is similar or better, compared to INCA. In contrast, the MSE between inverse and observed rainfall is generally higher compared to POBS and INCA and exhibits a higher variability in the single years.~~

→ Approximate location of Fig.13

~~Compared to ground observations and INCA the variance of the inverse rainfall is considerably higher for all aggregation lengths and periods (Fig. 14 (a) — (c)). Although the rainfall sums of the individual years are very similar (Fig. 10), the higher variance leads to higher MSE values of the inverse rainfall compared to observed rainfall. The variance of POBS and INCA is mostly very similar, explaining the comparatively lower MSE values between POBS and INCA.~~

→ Approximate location of Fig.14

Formatiert: Listenabsatz, Aufgezählt + Ebene: 1 +
Ausgerichtet an: 0.63 cm + Einzug bei: 1.27 cm

4.3.3 Rainfall and runoff simulations for a flood event

Fig. 45-12 exemplarily illustrates the temporal development of the different rainfall realisations and runoff simulations for the highest flood event in the ~~simulation period~~Krems catchment. Results from Exp3 are shown. Compared to ~~the ground observation~~POBS_PObs and ~~INCA-PI~~ncal the inverse rainfall P_{Inv} exhibits a higher variability and higher intensities. The higher variability and oscillating nature of the inverse rainfall is explainable with the reaction of the inverse model to small fluctuations in runoff observations: In case of rising runoff observations, rainfall will be estimated by the inverse model. If the observed runoff decreases and the simulated runoff of the inverse model is larger than observed runoff, no inverse rainfall will be calculated, leading to the visible oscillations. Fig. 45-12 (b) shows, that the forward model, driven with ~~POBS_PObs~~ as input, underestimates both flood peaks. The forward model, driven with the inverse rainfall, simulates ~~both the driven periods~~peaks very well (Inverse QS~~im~~IM). However, especially the falling limb after the second flood peak on the 07.09.2007 is overestimated by the inverse model. In this period it is also visible, that ~~in consequence~~ no rainfall is calculated by the inverse model, ~~since simulated runoff is higher than observed runoff~~.

→ Approximate location of Fig. 45-12

For a given time interval, the inverse model will yield an exact agreement between observed and simulated runoff, as long as there is a positive rainfall value R_t to solve eq. (5). This will be the case in periods of rising limbs of observed runoff (driven periods), as a rainfall value can be estimated, which raises the simulated runoff value to match observation. On the contrary, in periods of observed falling limbs (non-driven periods) the simulated runoff will solely be a function of the model structure, its parameters and the antecedent system states, as negative rainfall values are ruled out beforehand. This explains, why in periods, in which the simulated runoff is higher than the observed value, no rainfall is calculated by the inverse model.

4.1.2 Validation period

~~It can be argued, that the inverse rainfall is conditioned by the model parameter set from the calibration period, since the inverse rainfall shown in the preceding section was simulated with these parameters. The conclusion would be, that the performance of the inverse model to estimate rainfall in an independent period will deteriorate. This objection is absolutely~~

Formatiert: Englisch (Großbritannien)

Formatiert: Überschrift 3, Keine Aufzählungen oder Nummerierungen

legitimate, since model performance in classical rainfall runoff modelling frequently deteriorates in independent validation periods. The following results therefore show the inverse rainfall calculation for the independent validation period in the year 2009. The cumulative curves for the different rainfall realisations (Fig. 16) show a very similar behaviour compared to the data of 2006 to 2008 (see Fig. 10). Although there is a considerable deviation between the inverse rainfall and POBS curve at the end of the simulation period, the inverse rainfall matches quite well with the INCA data. This behaviour is very comparable to the year 2006 in the calibration period (see Fig. 10).

→ Approximate location of Fig.16

The correlation values between POBS and Inverse P in the validation period shown in Fig. 17 are comparable to the values of the calibration period (see Fig. 11). No obvious deterioration of the model performance is evident, leading to the conclusion that the model parameters were not strongly conditioned by the runoff conditions in the calibration period.

→ Approximate location of Fig.17

4.1.3 Exp5: Influence of different parameter optimisation data basis

The model parameters used for the forward and inverse model were automatically calibrated using the ground observation POBS as input. It could therefore be concluded that the model parameters are conditioned by POBS and that in consequence the good agreement between POBS and inverse P originates from this conditioning. Based on this hypothesis, calibrating the model with INCA data should lead to a better agreement between the INCA data and the corresponding inverse rainfall and a deterioration of the correlation between station data and inverse rainfall. To test this hypothesis, the forward model was automatically calibrated with INCA data as input and the resulting parameters set was then used to calculate the inverse rainfall. Based on the results shown in Fig. 18 this hypothesis can however be rejected. Although the correlation values between POBS and inverse P based on the POBS as calibration input are slightly higher compared to the inverse P values based on the INCA data calibration, the correlation values between INCA and the two different Inverse P realisations do not show noticeable differences.

→ Approximate location of Fig.18

It can therefore be concluded that agreement between POBS and inverse P is of similar magnitude, when simulating catchment rainfall with model parameters calibrated with the INCA data as input. This excludes that the parameters are conditioned by the input used for calibration.

4.1.44.3.4 Exp6: Influence of cold system states on the inverse rainfall (Exp6)

Given the model structure, the inverse rainfall is a function of observed runoff, potential evapotranspiration, system states and model parameters (see eq. (4)). Extending eq. (4) explicitly with all relevant system states (see Table. 4) leads to

$$R_t = f^{-1}(Q_t, ET_{p,t}, BW1_{t-1}, BW2_{t-1}, BW3_{t-1}, BW4_{t-1} | \theta_t) \quad (7)$$

Given eq. (7) it is conceivable, that the inverse rainfall R_t may be over-determined, meaning that different combinations of system states BW_i can lead to the same inverse rainfall estimates and that the results would not be unique. The forward and inverse models are run as a continuous simulation in time (Fig. 2). The preceding system states are therefore an integral part of the simulation and are determined intrinsically within the simulation. However, the initial system states at the beginning of the simulation period (cold states) will influence the results of the simulation, but should, after an adequate spin-up time, not influence the inverse rainfall estimates. To evaluate the influence of cold states on the inverse rainfall a virtual experiment was set up, in which 3 different cold start scenarios were defined:

- Reference scenario
- Dry system states scenario
- Wet system states scenario

For the reference scenario the system states of the 31.12.2008 from the continuous simulation were used. For the cold states in the dry scenario the states from the reference scenario were reduced by the factor 0.5 and increased by the factor 1.5 for the wet scenario.

To test the influence of cold states on the inverse rainfall simulations the simulation experiment Exp6 was performed. Three different cold states (Reference, dry and wet system states) were thereby defined (see section 2.3.2). From Fig. 49-13 exemplarily shows the results of Exp6 for the Krems catchment.

- Approximate location of Fig.13

Feldfunktion geändert

Formatiert: Listenabsatz, Aufgezählt + Ebene: 1 +
Ausgerichtet an: 0.63 cm + Einzug bei: 1.27 cm

890 ~~From showing~~ the monthly rainfall sums of the different model runs it is evident, that the
891 inverse rainfall calculations differ significantly at the beginning of the simulation. ~~The~~
892 ~~simulations were performed in a temporal resolution of 60 min, and only the results~~
893 ~~aggregated to monthly values for visualisation purposes.~~ In the first month the reference
894 scenario results in a monthly rainfall sum of 30 mm, the dry scenario in 111 mm and the wet
895 scenario in only 9 mm. Generally the model will always strive towards an equilibrium in its
896 system states, which are a function of the model structure and parameters. In the scenario
897 “wet” a lot of water is stored in the states of the model at the beginning, with the result, that
898 little inverse rainfall is calculated. In the dry scenario on the other hand a higher amount of
899 rainfall is estimated, since less water is stored in the states at the beginning. With time,
900 however, the different ~~system states converge~~~~inverse rainfall estimates will converge.~~ In ~~this~~
901 ~~timeconsequence~~ also the ~~system states~~~~inverse rainfall values~~ converge and after 9 months no
902 differences are evident.

903 → ~~Approximate location of Fig. 19~~

904 ~~Similar As in to classical rainfall runoff forward~~ models formulated in a state-space approach,
905 it is evident that cold states have a noteworthy influence on the simulation results. After an
906 adequate spin-up time the system states however converge, leading to deterministic and
907 unique inverse rainfall estimates.

908 **5 Summary ~~and conclusions~~ and outlook ~~conclusions~~**

909 A calibrated rainfall-runoff model (forward model) reflects the catchment processes leading to
910 runoff generation. Thus, inverting the model, i.e. calculating rainfall from runoff, yields the
911 temporally disintegrated rainfall. In this paper we applied a conceptual rainfall-runoff model,
912 which is inverted in an iterative approach, to simulate catchment rainfall from observed
913 runoff. The estimated inverse rainfall is compared with two different rainfall realisations:
914 Apart of ~~a~~-ground observations, areal rainfall fields of the INCA-system are used. ~~INCA is the~~
915 ~~meteorological nowcasting and analysis system developed and run by the Central Institute for~~
916 ~~Meteorology and Geodynamics of Austria (ZAMG) and is used for the majority of real-time~~
917 ~~flood forecasting systems in Austria. The approach is applied to two study areas in Austria.~~
918 ~~Hourly data is available for the years 2006 to 2009. Only the months of June to September are~~
919 ~~used, as the inverse model can only be applied in periods, in which runoff is not influenced by~~
920 ~~snow melt (i.e. summer months).~~

Formatiert: Englisch (Großbritannien)

In a first step, the forward model is calibrated ~~with the ground observation~~ against runoff observations. To evaluate the influences of (i) different model parameters due to different calibration periods and lengths, (ii) different runoff observations, and (iii) different parameter optimisation data basis on the runoff and rainfall calculations, several simulation experiments are performed. Additionally the influence of different initial conditions on the rainfall simulations are evaluated.

The forward model ~~and~~ mostly shows stable results in both catchments and reproduces the dynamics and variability of the catchment responses to rainfall in a satisfactory manner. ~~Comparable model performance is also found in the validation period. Only the simulation experiment, in which a single summer was used for parameter calibration, shows a larger deterioration of the model performance in the independent years.~~ These model parameters are then used for deriving catchment rainfall from runoff observations.

The cumulative rainfall curves of the ~~three~~ rainfall realisations (ground observation (POBS), INCA (PINCA) and inverse rainfall ~~from the different simulation experiments (Inverse PPIInv)~~) are very similar, suggesting, that the inverse model is capable of representing the long-term quantitative rainfall conditions of the catchment. About 60 % (Schliefau) and 45% (Krems) of rainfall is lost to the atmosphere due to actual evapotranspiration (ETa/AET). If the model would not capture ETa/AET adequately, the cumulative rainfall curves would not follow the observations so closely.

The correlation between ~~Inverse PPIInv~~ and ~~POBS-PObs~~, although rather low, is higher or of the same magnitude compared to the correlation between ~~POBS-PObs~~ and ~~INCA-PINCA~~, suggesting that the inverse model also reflects the timing of rainfall in equal quality of INCA. ~~The correlation between -PInv and PObs is mostly stable in the single years, independent of the simulation experiment. However, again for the simulation experiment with only a single summer for parameter calibration, a larger spread in the correlation for the single years is visible. An increase in observed runoff (Exp4) does not show negative effects on the inverse rainfall measured by the correlation coefficient. A larger bias between observed and modelled rainfall is however visible in Exp4. Generally, the simulation experiment with the highest performance in the runoff simulation also shows the highest correlation values in the rainfall simulations.~~

~~Quantitative differences in the rainfall realisations evaluated with the mean squared error (MSE) show significant larger errors between POBS and Inverse P compared to POBS and~~

~~INCA. Although the cumulative curves of the rainfall realisations are very similar, the higher variance of the inverse rainfall leads to the higher quantitative errors when evaluating the MSE. The higher variance to a great extent originates from a partial oscillating character of the inverse rainfall. Similar results are found for the validation period.~~

To test, if the inverse rainfall is conditioned by observed rainfall used as calibration input, additional model calibration is conducted using the INCA data as driving rainfall input for the forward model calibration. The simulation of inverse rainfall on the basis of this model parameters set show ~~very~~ similar results as before, suggesting, that the inverse rainfall is not conditioned to the rainfall input used for model calibration.

Since the inverse model is formulated in a state-space approach additional simulations are performed with differing cold states at the beginning of the simulations. Here the results show, that the resulting inverse rainfall values converge to identical values after an adequate spin-up time.

Generally, the results do not differ substantially between the two test catchments. It can be concluded that the application of the inverse model is a feasible approach to estimate mean areal rainfall values. The mean areal rainfall values can be used to enhance interpolated rainfall fields, e.g. for the estimation of rainfall correction factors or the parameterisation of elevation dependency. With the inverse model, it is not possible to calculate solid rainfall. In rainless periods, where it is clear, that snow melt is dominating runoff (e.g. in spring), the inverse model can however be used to quantify the snow melt contribution.

The estimation of areal rainfall leading to extreme flood events is afflicted with major uncertainties. Here the inverse modelling approach can be used as an additional information source concerning the rainfall conditions during extreme events. FurthermoreIn this context, it is conceivable to use the inverse model in real-time flood forecasting systems, ~~e.g. to gain additional information on rainfall quantities.~~ Here two different applications of the inverse model are conceivable:

1. A frequent problem observed in real-time flood forecasting models with state space formulations is that the system states in the models are biased in such a way that the simulated and observed runoff differ systematically. Methods exist to cope with this problem and to update the system states (e.g. Liu et al, 2012; McLaughlin, 2002). The system states in the inverse model will, at least during driven periods, always guarantee, that the simulated runoff

Formatiert: Englisch (Großbritannien)

is identical to observations. This fact may be used as a basis for updating system states in the flood forecasting models.

2. At least in Austria, 2 different types of precipitation forecasts are used as input in flood or runoff forecasting models - nowcasting fields (used for forecasts of $t=+1h$ to $t=+6h$) and fields from numerical weather forecasting models (used for $t>+6h$). The nowcasting fields strongly depend on the quality of station observations ($t=0h$), as they are the basis for extrapolation into the future (Haiden et al., 2011). By assimilating the inverse rainfall into the nowcasting system, i.e. to gain additional information on rainfall quantities, it is conceivable that the rainfall estimates of $t=0h$ can be improved. An extrapolation of the improved rainfall fields could therefore improve the nowcasting fields and in consequence the runoff forecasts.

There are however several methodological issues to be solved, before an application in this context is possible. These include the spatial disaggregation of the inverse rainfall and system states in case the flood forecasting models are set up as distributed models or the limitation of the inverse model, when used to calculate rainfall, to snow-free periods. Additionally, the application presented here focused on headwater basins. In this context, the estimation of rainfall from intermediate catchments is also a future challenge.

~~The estimation of areal rainfall leading to extreme flood events is afflicted with major uncertainties. Here the inverse modelling approach can be used as an additional information source concerning the rainfall conditions during extreme events.~~

In the presented work ~~two several~~ different model parameter sets were used as a basis to calculate inverse rainfall. In ~~a next step~~ further works the influences and uncertainties in the inverse rainfall, which arise from different model parameters ~~must~~ should be analysed systematically. ~~With this analysis as a basis the application of the inverse model in ungauged basins is conceivable.~~ Additionally, a comparison of inverse rainfall estimates from a different model structure for the two catchments with our results would be of interest, in order to check the ~~possible~~ links between the performance of the forward model and the results obtained by the inversion method. ~~Due to the lumped model setup only mean areal values of rainfall are calculated with the inverse model. The spatial disaggregation of the inverse areal rainfall estimates is therefore also an interesting future task.~~

Formatiert: Überschrift 1

1014 **Appendix**

1015 The forward model is formulated as follows, considering parameters and variables in Table 2
 1016 and Table 3:

1017
$$BWI_t = \max(\min(INTMAX, BWI_{t-1} + 0.5 * R_t - ETI_t), 0) = \max(\min(INTMAX, BWI_{t-1} + 0.5 * R_t - f(ETp_t, INTMAX)), 0) \quad (A1)$$

1018
$$R_Soil_t = 0.5 * R_t + \max(BWI_{t-1} + 0.5 * R_t - ETI_t - INTMAX, 0) \quad (A2)$$

1019
$$BW0_t = BW0_{t-1} + R_Soil_t - ETG_t - Q1_t - Q2_t = BW0_{t-1} + R_Soil_t - \min\left(\frac{BW0_{t-1}}{FKFAK * M}, 1\right) * (ETp_t - ETI_t) * ETVEGCOR - R_Soil_t * \left(\frac{BW0_{t-1}}{M}\right)^{BETA} - f(PEX2) * BW0_{t-1} \quad (A3)$$

1020
$$BW2_t = BW2_{t-1} + Q2_t - QAB2_t - QVS2_t = BW2_{t-1} + f(PEX2) * BW0_{t-1} - \alpha_2 * \max(BW2_{t-1} - H2, 0) - \beta_2 * BW2_{t-1} \quad (A4)$$

1021
$$BW3_t = BW3_{t-1} + QVS2_t - QAB3_t = BW3_{t-1} + \beta_2 * BW2_{t-1} - \alpha_3 * BW3_{t-1} \quad (A5)$$

1022
$$BW4_t = BW4_{t-1} + Q1_t + QAB2_t + QAB3_t - QSIM_t = BW4_{t-1} + R_Soil_t * \left(\frac{BW0_{t-1}}{M}\right)^{BETA} + \alpha_2 * \max(BW2_{t-1} - H2, 0) + \alpha_3 * BW3_{t-1} - \alpha_4 * BW4_{t-1} \quad (A6)$$

1023 with

1024
$$\alpha_i = \frac{\Delta t}{TAB_i} \quad \text{and} \quad (A7)$$

1025
$$\beta_i = \frac{\Delta t}{TVS_i} \quad (A8)$$

1026 The forward model is formulated as follows, considering parameters and variables in Table 2
 1027 and Table 3:

1028
$$BWI_t = \max(\min(INTMAX, BWI_{t-1} + R_t - ETp_t), 0) \quad (A1)$$

Feldfunktion geändert

Formatiert: Englisch (Großbritannien)

$$BW0_t = BW0_{t-1} + R_t - ETG_t - Q1_t - Q2_t =$$

$$BW0_{t-1} + R_t - \min\left(\frac{BW0_{t-1}}{FKFAK * M}, 1\right) * ETp_t * ETVEGCOR - R_t * \left(\frac{BW0_{t-1}}{M}\right)^{BETA} - f(PEX2) * BW0_{t-1}$$

(A2)

$$BW2_t = BW2_{t-1} + Q2_t - QAB2_t - QVS2_t =$$

$$BW2_{t-1} + PEX2 * BW0_{t-1} - \alpha_2 * \max(BW2_{t-1} - H2, 0) - \beta_2 * BW2_{t-1}$$

(A3)

Formatiert: Englisch (Großbritannien)

$$BW3_t = BW3_{t-1} + QVS2_t - QAB3_t = BW3_{t-1} + \beta_2 * BW2_{t-1} - \alpha_3 * BW3_{t-1}$$

(A4)

Formatiert: Englisch (Großbritannien)

$$BW4_t = BW4_{t-1} + Q1_t + QAB2_t + QAB3_t - QSIM_t =$$

$$BW4_{t-1} + R_t * \left(\frac{BW0_{t-1}}{M}\right)^{BETA} + \alpha_2 * \max(BW2_{t-1} - H2, 0) + \alpha_3 * BW3_{t-1} - \alpha_4 * BW4_{t-1}$$

(A5)

Formatiert: Englisch (Großbritannien)

with

$$\alpha_i = \frac{\Delta t}{TAB_i} \text{ and}$$

(A6)

Formatiert: Englisch (Großbritannien)

$$\beta_i = \frac{\Delta t}{TVS_i}$$

(A7)

Formatiert: Englisch (Großbritannien)

TAB_i / TVS_i = recession coefficients. Δt = modelling time step in units of hours. α and β vary with modelling time step and represent smoothing functions of the linear reservoirs

Formatiert: Englisch (Großbritannien)

Eq. A1 to A8 are simplified representations of the model algorithm. Min/max operators, which, by introducing discontinuities, can lead to non-inversibility. Eq. A4 and A6 do not include a threshold function in the actual model code. The differential equations of the linear reservoirs are solved analytically. An internal time step discretization is included in the code, to guarantee, that the transition between system states above and below the threshold value is solved exactly. A3, representing the soil layer, does include a min() operator for estimating the ratio between actual and potential evapotranspiration as a function of soil water content. This is however not a limiting factor for the inversion, since this factor is a function of the preceding soil state BW0_{t-1}, which is known. Only 50% of rainfall is used as input into the interception storage BWI. By assuming that the other 50% are always throughfall, eq. A1 and A2 also does not limit the inversion, since a continuous signal through the whole model cascade is guaranteed. The recession coefficient representing percolation processes in the soil

1054 layer exhibits a nonlinear characteristic and is calculated as a function of actual soil water
1055 content and a as a function of the form parameter PEX2 [-]. This model concept reflects the
1056 fact, that higher soil moisture levels lead to higher soil permeability values. These induce
1057 higher percolation rates which are reflected by lower recession coefficients. ~~The normalised~~
1058 ~~curves in Fig. A1 are based on the equation for the soil water content pressure head curve~~
1059 ~~presented by Van Genuchten (1980), where n in the original equation is represented by PEX2~~
1060 ~~[-].~~

1061 ➔ ~~Approximate location of Fig. A1~~

1062

Formatiert: Englisch (Großbritannien)

Formatiert: Standard, Keine Aufzählungen oder
Nummerierungen

Formatiert: Überschrift 1

1063 References

- 1064 Ahrens, B., Jasper, K., and Gurtz, J.: On ALADIN rainfall modeling and validation in an
 1065 Alpine watershed—, Annales-Ann. GeophysicaeGeophys., 21, 627–637, [doi:10.5194/angeo-](https://doi.org/10.5194/angeo-21-627-2003)
 1066 [21-627-2003](https://doi.org/10.5194/angeo-21-627-2003), 2003.
- 1067 Bergström, S.: The HBV model, in: Computer Models of Watershed Hydrology, edited by:
 1068 Singh, V. P., Water Resources Publications, Highland Ranch, CO, USA, 443–476,
 1069 1995, Singh, V.P. (Ed.), Computer Models of Watershed Hydrology, Water Resources
 1070 Publications, Highland Ranch CO, USA, pp. 443–476, 1995.
- 1071 Bica, B., Hermegger, M., Kann, A., and Nachtnebel, H. P.: HYDROCAST – Enhanced
 1072 Estimation—estimation of Areal—areal Rainfallrainfall by Combining—combining a
 1073 Meteorological—meteorological Noweasting—nowcasting System—system with a Hydrological
 1074 hydrological Modelmodel—, Final Report, Austrian Academy of Science, Vienna,—
 1075 Doi[doi:10.1553/hydrocast2011](https://doi.org/10.1553/hydrocast2011), 2011.
- 1076 BMLFUW: Hydrological Atlas of Austria, 3rd Edn., Bundesministerium für Land- und
 1077 Forstwirtschaft, Umwelt und Wasserwirtschaft, Wien, ISBN: 3-85437-250-7, 2007.
- 1078 BMLFUW: Hydrographical yearbook of Austria—, Abteilung VII 3 - Wasserhaushalt im
 1079 Bundesministerium für Land und Forstwirtschaft, Umwelt und Wasserwirtschaft, Wien, 2009.
- 1080 BMLFUW: Hydrological Atlas of Austria, third ed. Wien: Bundesministerium für Land- und
 1081 Forstwirtschaft, Umwelt und Wasserwirtschaft. ISBN: 3-85437-250-7, 2007.
- 1082 Brent, R.P.: Algorithms for Minimization without Derivatives—, Prentice-Hall, Englewood
 1083 Cliffs, NJ: Prentice Hall, 1973.
- 1084 de Jong, C., List, F., and Ergenzinger, C.: Experimental hydrological analyses in the Dischma
 1085 based on daily and seasonal evaporation—, Nord. Hydrol. 33(+), 1–14, 2002.
- 1086 Di Baldassarre G., and Montanari, A.: Uncertainty in river discharge observations: a
 1087 quantitative analysis—, Hydrol. Earth Syst. Sci., 13(6), 913–921, [doi:10.5194/hess-13-913-](https://doi.org/10.5194/hess-13-913-2009)
 1088 [2009](https://doi.org/10.5194/hess-13-913-2009), 2009.
- 1089 Duan, Q., Sorooshian, S., and Gupta, V.K.: Effective and Efficient Global Optimization for
 1090 Conceptual Rainfall-runoff Models—, Water Resour. Res., 28(4), 1015–1031, 1992.

Formatiert: Englisch (Großbritannien)

Formatiert: Deutsch (Österreich)

Formatiert: Deutsch (Österreich)

1091 Eder, G., Fuchs, M., Nachtnebel, H.P., and Loibl, W.: Semi-distributed modelling of the
1092 monthly water balance in an alpine catchment—, *Hydrol. ~~Processes~~ Process.* 19, 2339–2360,
1093 2005.

1094 Elias, V., Tesar, M., and Buchtele, J.: Occult precipitation: sampling, chemical analysis and
1095 process modeling in the Sumava Mts. (Czech Republic) and in the Taunus Mts. (Germany),
1096 *J. Hydrol.* 166 ~~(1995)~~, 409–420, 1995.

1097 Fekete, B.M., Vorosmarty, C.J., Roads, J.O., and Willmot, C.J.: Uncertainties in precipitation
1098 and their impacts on runoff estimates, *J. Clim.* 17, 294– 304, 2004.

1099 Goodison, B.E., Louie, P.Y.T., and Yang, D.: WMO solid precipitation measurement
1100 intercomparison, Instruments and Observing Methods Rep. 67 (WMO/TD 872), World
1101 Meteorological Organization, Geneva, Switzerland, 318 pp, 1998.

1102 Groetsch, C.: Inverse Problems in Mathematical Sciences, Vieweg Mathematics for Scientists
1103 and Engineers, Wiesbaden, 1993.

1104 Haiden, T., and Pistotnik, G.: Intensity-dependent parameterization of elevation effects in
1105 precipitation analysis, *Adv. Geosci.*, 20, 33–38, doi:10.5194/adgeo-20-33-2009, 2009.

1106 Haiden, T., Kann, A., Wittman, C., Pistotnik, G., Bica, B., and Gruber, C.: The Integrated
1107 Nowcasting through Comprehensive Analysis (INCA) system and its validation over the
1108 Eastern Alpine region—, *Weather Forecast.*, 26, 166–183, doi:10.1175/2010WAF2222451.1,
1109 2011. ~~Wea. Forecasting~~ 26, 166–183, doi: 10.1175/2010WAF2222451.1, 2011.

1110 ~~Haiden, T., and Pistotnik, G.: Intensity dependent parameterization of elevation effects in~~
1111 ~~precipitation analysis. *Adv. Geosci.* 20, 33–38, 2009.~~

1112 Hargreaves, G.H., and Samani, Z.A.: Estimating potential evapotranspiration—, *J. ~~Irrigation~~*
1113 *~~Irr. Drainage~~ Drain. Div-ASCE.*, 108, 225–230, 1982.

1114 Herrnegger, M.: Zeitlich hochaufgelöste inverse Modellierung von Gebietsniederschlägen aus
1115 Abflussmessungen, *PhD thesis, Institute of Water Management, Hydrology and Hydraulic*
1116 *Engineering, University of Natural Resources and Life Sciences, Vienna, Austria* ~~(in~~
1117 ~~German)~~, 2013.

1118 Herrnegger, M., Nachtnebel, H.P., and Haiden, T.: Evapotranspiration in high alpine
1119 catchments - an important part of the water balance!, *Hydrol. Res.* ~~2012~~; 43~~(4)~~; 460-475,
1120 2012.

1121 Hino, M., and Hasabe, M.: Analysis of hydrologic characteristics from runoff data – ~~A-a~~
1122 hydrologic inverse problem. J. Hydrol., 49, 287-313, 1981.

1123 Jacobs, A.F.G., Heusinkveld, B.G., and Wichink Kruit, R.J.: Contribution of dew to the water
1124 budget of a grassland area in the Netherlands—, Water Resour. Res., 42, W03415,
1125 doi:10.1029/2005WR004055, 2006.

1126 Jasper, K. and Kaufmann, P.: Coupled runoff simulations as validation tools for atmospheric
1127 models at the regional scale. Q. J. Roy. Meteorol. Soc., 129, 673-692, 2007.

1128 Jasper, K., Gurtz, J., and Lang, H.: Advanced flood forecasting in Alpine watersheds by
1129 coupling meteorological observations and forecasts with a distributed hydrological model—, J.
1130 Hydrol., 267, 40-52, 2002.

1131 ~~Jasper, K., Kaufmann, P.: Coupled runoff simulations as validation tools for atmospheric~~
1132 ~~models at the regional scale. Q.J.R. Meteorol. Soc., 129, 673-692, 2007.~~

1133 Kirchner, J._W.: Catchments as simple dynamical systems: Catchment characterization,
1134 rainfall-runoff modeling, and doing hydrology backward—, Water Resour. Res., 45, W02429,
1135 doi:10.1029/2008WR006912, 2009.

1136 Klemm, O., and Wrzesinski, T.: Fog deposition fluxes of water and ions to a mountainous site
1137 in Central Europe—, Tellus 59, 705-714, 2007.

1138 Kling, H.: Spatio-temporal modelling of the water balance of Austria. Dissertation, University
1139 of Natural Resources and Applied Life Sciences, 234 pp., available at:
1140 <http://iwhw.boku.ac.at/dissertationen/kling.pdf> (last access: 7 October 2014), 2006.

1141 Kling, H., and Nachtnebel, H.P.: A method for the regional estimation of runoff separation
1142 parameters for hydrological modelling, J. Hydrol., 364, 163–174, 2009.

1143 Kling, H., Stanzel, P., Fuchs, M., and Nachtnebel, H.P.: Performance of the COSERO
1144 precipitation-runoff model under non-stationary conditions in basins with different climates,
1145 Hydrolog. Sci. J., doi: 10.1080/02626667.2014.959956, in press, 2015.~~in press, 2014.~~

1146 Krajewski, W.F., and Smith, J.A.: Radar hydrology: rainfall estimation, Adv. Water Resour.,
1147 25, 1387-13, 2002.

1148 Krajewski, W.F., Villarini, G., and Smith, J.A.: RADAR-rainfall uncertainties, B. Am.
1149 Meteorol. Soc., 91, 87–94. doi:10.1175/2009BAMS2747.1, 2010

1150 [Krier, R., Matgen, P., Goergen, K., Pfister, L., Hoffmann, L., Kirchner, J. W., Uhlenbrook, S.,](#)
1151 [and Savenije, H.H.G.: Inferring catchment precipitation by doing hydrology backward: A test](#)
1152 [in 24 small and mesoscale catchments in Luxembourg, Water Resour. Res., 48, W10525,](#)
1153 [doi:10.1029/2011WR010657, 2012.](#)
1154 Kuczera, G., Kavetski, D., Franks, S., and Thyer, M.: Towards a Bayesian total error analysis
1155 of conceptual rainfall-runoff models: Characterising model error using storm-dependent
1156 parameters—J. Hydrol., 331(1–2), 161–177, 2006.
1157 Kunstmann, H., and Stadler, C.: High resolution distributed atmospheric-hydrological
1158 modeling for Alpine catchments—J. Hydrol., 314, 105–124, 2005.
1159 [Liu, Y., Weerts, A. H., Clark, M., Hendricks Franssen, H.-J., Kumar, S., Moradkhani, H.,](#)
1160 [Seo, D.-J., Schwanenberg, D., Smith, P., van Dijk, A. I. J. M., van Velzen, N., He, M., Lee,](#)
1161 [H., Noh, S. J., Rakovec, O., and Restrepo, P.: Advancing data assimilation in operational](#)
1162 [hydrologic forecasting: progresses, challenges, and emerging opportunities. Hydrol. Earth](#)
1163 [Syst. Sci., 16, 3863–3887, 2012.](#)
1164 [McLaughlin, D.: An integrated approach to hydrologic data assimilation: interpolation,](#)
1165 [smoothing and filtering. Advances in Water Resources, 25, 1275–1286, 2002.](#)
1166 ~~[Krajewski, W.F., and Smith, J.A.: Radar hydrology: rainfall estimation. Adv. Water](#)~~
1167 ~~[Resources, 25, 1387–13, 2002.](#)~~
1168 ~~[Krajewski, W.F., Villarini, G., and Smith, J.A.: RADAR Rainfall Uncertainties. Bull. Amer.](#)~~
1169 ~~[Meteor. Soc., 91, 87–94. doi: <http://dx.doi.org/10.1175/2009BAMS2747.1>, 2010](#)~~
1170 ~~[Krier, R., Matgen, P., Goergen, K., Pfister, L., Hoffmann, L., Kirchner, J. W., Uhlenbrook, S.,](#)~~
1171 ~~[and Savenije, H.H.G.: Inferring catchment precipitation by doing hydrology backward: A test](#)~~
1172 ~~[in 24 small and mesoscale catchments in Luxembourg, Water Resour. Res., 48, W10525,](#)~~
1173 ~~[doi:10.1029/2011WR010657, 2012.](#)~~
1174 McMillan, H., Freer, J., Pappenberger, F., Krueger, T., and Clark, M.: Impacts of uncertain
1175 river flow data on rainfall-runoff model calibration and discharge predictions—J. Hydrol.
1176 Process., 24, 1270–1284, doi:10.1002/Hyp.7587, 2010.
1177 [Nachtnebel, H. P., Herrnegger, M., Kahl, B., and Hepp, G.: Meteorologisch-hydrologisches](#)
1178 [Warnsystem Steyr: Endbericht und Technische Dokumentation - Teil 3 - Hydrologische](#)

1179 Abflussmodellierung, Amt der OÖ Landesregierung - Abteilung Wasserwirtschaft,
1180 Schutzwasserwirtschaft und Hydrographie, 197, 2010a.

1181 Nachtnebel, H.P., Senoner, T., Kahl, B., Apperl, B., and Waldhör, B.:
1182 Hochwasserprognosesystem Ybbs - Hydrologische Abflussmodellierung, Amt der NÖ
1183 Landesregierung, St. Pölten, 176, 2010b.

1184 Nachtnebel, H.P., Haberl, U., Stanzel, Ph., Kahl, B., Holzmann, H., and Pfaffenwimmer, Th.:
1185 Hydrologische Abflussmodellierung - Teil 3, in: Amt der Salzburger Landesregierung:
1186 HydriisII Hydrologisches Informationssystem zur Hochwasservorhersage im Land Salzburg,
1187 Amt der Salzburger Landesregierung, 341, 2009a.

1188 Nachtnebel, H. P., Senoner, T., Stanzel, P., Kahl, B., Hernegger, M., Haberl, U. and
1189 Pfaffenwimmer, T.: Inflow prediction system for the Hydropower Plant Gabčíkovo, Part 3 -
1190 Hydrologic Modelling, Slovenské elektrárne, a.s. Bratislava, 139, 2009b.

1191 Nachtnebel, H.P., Baumung, S., and Lettl, W.: Abflussprognosemodell für das Einzugsgebiet
1192 der Enns und Steyr, ~~(in German): Reportreport,~~ Institute of Water Management, Hydology
1193 and Hydraulic Engineering, University of Natural Resources and Applied Life Sciences,
1194 Vienna, Austria, 1993.

1195 Nash, J. E., and Sutcliffe, J. V.: River flow forecasting through conceptual models--Part I: A
1196 discussion of principles--J. Hydrol., 10, 282–290, 1970.

1197 Pappenberger, F., Matgen, P., Beven, K.J., Henry J.B., Pfister, L., and de Fraipont, P.:
1198 Influence of uncertain boundary conditions and model structure on flood inundation
1199 predictions--Adv. Water Resour., 29, 1430–1449, 2006.

1200 Pelletier, M.P.: Uncertainties in the determination of river discharge: a literature review, Can.
1201 J. Civ. Eng., 15, 834–850, 1987.

1202 Perrin, C., Michel, C., and Andréassian, V.: Does a large number of parameters enhance
1203 model performance? Comparative assessment of common catchment model structures on 429
1204 catchments--J. Hydrol., 242, 275–301, 2001.

1205 Press, W.H., Teukolsky, S.A., Vetterling, W.T., and Flannery, B.P.: Numerical Recipes in
1206 FORTRAN, The Art of Scientific Computing, ~~965 pp.,~~ Cambridge Univ. Press, New York,
1207 965 pp., 1992.

Formatiert: Englisch (Großbritannien)

1208 Seibert, J.: Reliability of model predictions outside calibration conditions, Nord. Hydrol., 34,
1209 477–492, 2003.

1210 Seibert, J., and Morén, A.-S.: Reducing systematic errors in rainfall measurements using a
1211 new type of gauge—, Agric. Forest. Meteorol., 98–99, 341–348, 1999.

1212 Sevruck, B.: Methodische Untersuchungen des systematischen Messfehlers der Hellmann-
1213 Regenschirm im Sommerhalbjahr in der Schweiz—, Dissertation, Zürich, Eidgenöss. Techn.
1214 Hochsch., Dissertation, Zürich, Zürich, Switzerland, (in German), 1981.

1215 Sevruck, B.: Correction of precipitation measurements. Proc. Workshop on the Correction of
1216 Precipitation Measurements—, In: Zürcher Geographische Schriften, ETH Zürich Zürich, no.
1217 23 (1986), p. 289, 1986.

1218 Sevruck, B., and Nespor, V.: Empirical and theoretical assessment of the wind induced error of
1219 rain measurement—, Water Sci. Technol., 37(44), 171–178, 1998.

1220 Simoni, S., Padoan, S., Nadeau, D.F., Diebold, M., Porporato, A., Barrenetxea, G., Ingelrest,
1221 F., Vetterli, and M., Parlange, M.B.: Hydrologic response of an alpine watershed: Application
1222 application of a meteorological wireless sensor network to understand streamflow generation,
1223 Water Resour. Res., 47, W10524, doi:10.1029/2011WR010730, 2011.

1224 Stanzel, Ph., Kahl, B., Haberl, U., Herrnegger, M., and Nachtnebel, H. P.: Continuous
1225 hydrological modeling in the context of real time flood forecasting in alpine Danube tributary
1226 catchments, IOP Conference Series—Earth and Environmental Science, 4, 012005,
1227 doi:10.1088/1755-1307/4/1/012005; ISSN 1755-1315, 2008.

1228 Sugawara, M.: On the weights of precipitation stations. in: O’Kane, J.P. (Ed.), Advances in
1229 Theoretical Hydrology, edited by O’Kane, J.P., Elsevier Science Publishers, Amsterdam, pp.
1230 59–74, 19931992.

1231 Tarantola, A.: Inverse problem theory and methods for model parameter estimation—, Society
1232 for Industrial and Applied Mathematics—Philadelphia, 352 pp., 2005.

1233 Valéry, A., Andréassian, V., and Perrin, C.: Regionalisation of rainfall and air temperature
1234 over high-altitude catchments—learning from outliers. Hydrol. Sci. J. 55(6), 928–940, 2010.

1235 Valéry, A., Andréassian, V., and Perrin, C.: Inverting the hydrological cycle: when
1236 streamflow measurements help assess altitudinal precipitation gradients in mountain areas—,

Formatiert: Englisch (Großbritannien)

Formatiert: Deutsch (Österreich)

Formatiert: Deutsch (Österreich)

1237 ~~44in~~: New Approaches to Hydrological Prediction in Data-sparse Regions, ~~281-286~~. IAHS
1238 Publ., 333, ~~281-286, 2009. Available from: <http://iahs.info/redbooks/333.htm>, 2009.~~

1239 ~~Valéry, A., Andréassian, V., and Perrin, C.: Regionalisation of rainfall and air temperature~~
1240 ~~over high-altitude catchments – learning from outliers, Hydrol. Sci. J., 55, 928–940, 2010.~~

1241 van Genuchten, M.~~T~~~~h~~: A closed-form equation for predicting the hydraulic conductivity of
1242 unsaturated soils~~–~~. Soil Sci. Soc. Am J., 44, 892-898, 1980.

1243 Vrugt, J.A., ter Braak, C.J.F., Clark, M.P., Hyman, J.M., and Robinson B.A.: Treatment of
1244 input uncertainty in hydrologic modeling: ~~Doing-doing~~ hydrology backward with Markov
1245 chain Monte Carlo simulation, Water Resour. Res., 44, W00B09,
1246 doi:10.1029/2007WR006720, 2008.

1247 Wood, S.J., Jones, D.A., and Moore, R.J.: ~~Accuracy of rainfall measurement for scales of~~
1248 ~~hydrological interest, Hydrol. Earth Syst. Sci., 4, 531–543, doi:10.5194/hess-4-531-~~
1249 ~~2000. Accuracy of rainfall measurement for scales of hydrological interest, Hydrol. Earth Syst.~~
1250 ~~Se. 4(4), 531-543, 2000.~~

1251

Tables

Table 1: Magnitude of different systematic errors in precipitation measurements (Sevruk, 1981, 1986; Goodison et al., 1998; Elias et al., 1993; Jacobs et al., 2006; Klemm and Wrzesinsky, 2007).

Systematic error	Magnitude
Wind-induced errors	2 - 10 % (liquid precipitation) 10 - >50 % (snow)
Wetting losses	2 - 10 %
Evaporation losses	0 - 4 %
Splash-out and splash-in	1 - 2 %
Fog and dew	4 - 10 %

Systematic error	Magnitude
Wind-induced errors	2 - 10 % (liquid precipitation) 10 - >50 % (snow)
Wetting losses	2 - 10 %
Evaporation losses	0 - 4 %
Splash-out and splash-in	1 - 2 %
Fog and dew	4 - 10 %

Table 2: Model parameters θ_j . Parameters in *italics* are calibrated.

Parameter	Units	Range	Description
INTMAX	mm	0.5 - 2.5	Interception storage capacity
<i>M</i>	mm	80 - 250	Soil storage capacity
<i>FKFAK</i>	-	0.5 - 1	Critical soil moisture for actual evapotranspiration
ETVEGCOR	-	0.4 - 1.1	Vegetation correction factor for actual evapotranspiration from soil
<i>BETA</i>	-	0.1 - 10	Exponent for computing fast runoff generation
KBF	h	4000 - 12000	Recession coefficient for percolation from soil module
<i>PEX2</i>	-	5 - 25	Parameter for non-linear percolation
<i>TAB2</i>	h	50 - 500	Recession coefficient for interflow
<i>TVS2</i>	h	50 - 500	Recession coefficient for percolation from interflow reservoir
H2	mm	0 - 25	Outlet height for interflow
<i>TAB3</i>	h	1000 - 5000	Recession coefficient for base flow
<i>TAB4</i>	h	0.05 - 10	Recession coefficient for routing

Parameter	Units	Range	Description
INTMAX	mm	0.5 - 2.5	Interception storage capacity
<i>M</i>	mm	80 - 250	Soil storage capacity
<i>FKFAK</i>	-	0.5 - 1	Critical soil moisture for actual evapotranspiration
ETVEGCOR	-	0.4 - 1.1	Vegetation correction factor for actual evapotranspiration from soil
<i>BETA</i>	-	0.1 - 10	Exponent for computing fast runoff generation

Formatiert: Überschrift 1, Einzug: Links: 0.76 cm

Formatiert: Englisch (Großbritannien)

Formatiert: Englisch (Großbritannien)

Formatiert: Englisch (Großbritannien)

Formatiert: Englisch (Großbritannien)

Formatiert: Englisch (Großbritannien)

<i>KBF</i>	h	4000 - 12000	Recession coefficient for percolation from soil module
<i>PEX2</i>	-	5 - 25	Parameter for non-linear percolation
<i>TAB2</i>	h	50 - 500	Recession coefficient for interflow
<i>TVS2</i>	h	50 - 500	Recession coefficient for percolation from interflow reservoir
<i>H2</i>	mm	0 - 25	Outlet height for interflow
<i>TAB3</i>	h	1000 - 5000	Recession coefficient for base flow
<i>TAB4</i>	h	0.05 - 10	Recession coefficient for routing

1261

1262

1263

Table 3: Model fluxes and system states S_i . Fluxes represent sums over the time step.

Variable	Units	Type	Description
R	mm	Input	Rainfall
ETp	mm	Input	Potential evapotranspiration
ETI	mm	Ouput	Actual Evapotranspiration from interception module
ETG	mm	Ouput	Actual Evapotranspiration from soil module
BW1	mm	State	Water stored in interception module
BW0	mm	State	Water stored in soil module
BW2	mm	State	Water stored in interflow reservoir
BW3	mm	State	Water stored in baseflow reservoir
BW4	mm	State	Water stored in routing reservoir
R_Soil	mm	Internal flux	Input into soil module
Q1	mm	Internal flux	Fast runoff from soil module
Q2	mm	Internal flux	Percolation from soil module
QAB2	mm	Internal flux	Interflow
QVS2	mm	Internal flux	Percolation from interflow reservoir
QAB3	mm	Internal flux	Base flow
QSIM	mm	Output	Total runoff

1264

Variable	Units	Type	Description
R	mm	Input	Rainfall
ETp	mm	Input	Potential evapotranspiration
ETI	mm	Output	Actual Evapotranspiration from interception module
ETG	mm	Output	Actual Evapotranspiration from soil module
BW1	mm	State	Water stored in interception module
BW0	mm	State	Water stored in soil module
BW2	mm	State	Water stored in interflow reservoir
BW3	mm	State	Water stored in base flow reservoir
BW4	mm	State	Water stored in routing reservoir
R_Soil	mm	Internal flux	Input into soil module
Q1	mm	Internal flux	Fast runoff from soil module
Q2	mm	Internal flux	Percolation from soil module
QAB2	mm	Internal flux	Interflow
QVS2	mm	Internal flux	Percolation from interflow reservoir
QAB3	mm	Internal flux	Base flow
QSIM	mm	Output	Total runoff

1265

1266

Table 4: Characteristics of the study catchments (BMLFUW, 2007; BMLFUW, 2009).

	Schlieffau	Krems
Basin area [km ²]	17.9	38.4

Formatiert: Tiefgestellt

Formatiert: Englisch (Großbritannien)

Formatierte Tabelle

	<u>Mean elevation [m]</u>	<u>608</u>	<u>598</u>
	<u>Elevation range [m]</u>	<u>390 - 818</u>	<u>413 - 1511</u>
	<u>Mean annual precipitation [mm]</u>	<u>1390</u>	<u>1345</u>
	<u>Mean annual runoff [m³/s]</u>	<u>0.38</u>	<u>1.12</u>

1267

1268

1269 Table 5: Overview of the model calibration and simulations experiments with observed input
 1270 data. P_{eObs} and P_{Inca} refer to the rainfall from the station observations and the INCA
 1271 system.

	<u>June to Sept. Periods in year</u>				<u>Driving input (Forward / inverse model)</u>	<u>Purpose</u>
	<u>2006</u>	<u>2007</u>	<u>2008</u>	<u>2009</u>		
<u>Exp1</u>	<u>calib.</u>	<u>valid.</u>	<u>valid.</u>	<u>valid.</u>	<u>P_{eObs} / Q</u>	<u>Influence of different calibration periods on simulations</u>
<u>Exp2</u>	<u>calib.</u>	<u>calib.</u>	<u>valid.</u>	<u>valid.</u>	<u>P_{eObs} / Q</u>	
<u>Exp3</u>	<u>calib.</u>	<u>calib.</u>	<u>calib.</u>	<u>valid.</u>	<u>P_{eObs} / Q</u>	
<u>Exp4</u>	<u>calib.</u>	<u>calib.</u>	<u>calib.</u>	<u>valid.</u>	<u>$P_{eObs} / Q + 10\%$</u>	<u>Influence of different runoff Q on simulations</u>
<u>Exp5</u>	<u>calib.</u>	<u>calib.</u>	<u>calib.</u>	<u>valid.</u>	<u>P_{Inca} / Q</u>	<u>Influence of different rainfall input on simulations</u>
<u>Exp6</u>	<u>Parameters from Exp3, but different initial conditions</u>				<u>P_{eObs} / Q</u>	<u>Influence of initial conditions cold states on simulations</u>

Formatiert: Englisch (Großbritannien)

Formatiert: Englisch (Großbritannien)

1272
 1273

Table 6: Model performance for the different simulation experiments and the two catchments of the forward model, expressed by Nash-Sutcliffe-Efficiency (NSE) and the mean bias between simulated and observed runoff in percent of observed runoff for the period 2006 to 2009. Only the months June to ~~July, August and~~ September are evaluated.

		NSE [-]	mean BIAS [%]
Schliefau	Exp1	0.822	7.8
	Exp2	0.832	3.9
	Exp3	0.828	0.9
	Exp4	0.830	-5.9
	Exp5	0.728	-0.6
Krems	Exp1	0.763	-1.4
	Exp2	0.851	-4.8
	Exp3	0.851	-4.8
	Exp4	0.854	-7.9
	Exp5	0.787	1.5

Table 7: Correlation for 2006 to 2009 between different rainfall realisations and temporal aggregation lengths. (PObs: Ground observation, PInv: Inverse rainfall from Exp1 to Exp5, PInca: INCA rainfall). Only the months June, July, August and September are evaluated.

		CORR: 1h-sums			CORR: 6h-sums			CORR: 24h-sums		
		PObs - PInv	PInca - PInv	PObs - PInca	PObs - PInv	PInca - PInv	PObs - PInca	PObs - PInv	PInca - PInv	PObs - PInca
Schliefau	Exp1	0.504	0.251		0.800	0.671		0.871	0.802	
	Exp2	0.549	0.290		0.828	0.703		0.914	0.840	
	Exp3	0.534	0.284	0.463	0.824	0.699	0.849	0.918	0.845	0.928
	Exp4	0.530	0.283		0.818	0.695		0.917	0.843	
	Exp5	0.524	0.276		0.824	0.697		0.920	0.842	
Krems	Exp1	0.478	0.394		0.794	0.771		0.871	0.847	
	Exp2	0.517	0.445		0.831	0.807		0.909	0.889	
	Exp3	0.517	0.445	0.469	0.831	0.807	0.864	0.909	0.889	0.931
	Exp4	0.517	0.445		0.833	0.809		0.909	0.892	
	Exp5	0.503	0.445		0.820	0.805		0.901	0.888	

Formatierte Tabelle

Table 8: Mean Bias for 2006 to 2009 between different rainfall realisations.

		Mean Bias [mm/d]	
		PInv - PObs	PInca - PObs
Schliefau	Exp1	0.14	
	Exp2	0.07	
	Exp3	0.22	0.02
	Exp4	0.42	
	Exp5	0.33	
Krems	Exp1	0.28	
	Exp2	0.40	
	Exp3	0.40	0.47
	Exp4	0.53	
	Exp5	0.49	

Formatiert: Schriftart: 11 Pt.

Formatiert: Zentriert

Formatiert: Schriftart: 11 Pt.

Formatierte Tabelle

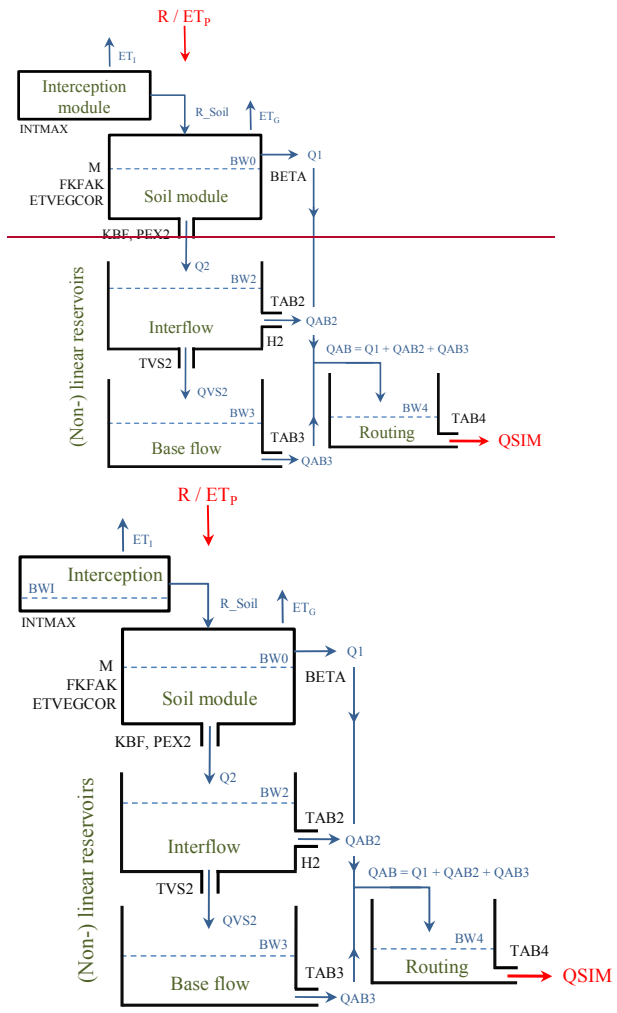
1287 **Figures**

1288

1289

1290

1291 Figure 1: Structure, parameters and states of the forward model.



Formatiert: Überschrift 1

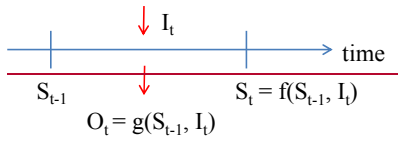


Figure 2: Schematic representation of the state space approach with system states S , Input I , Output O and time component t .

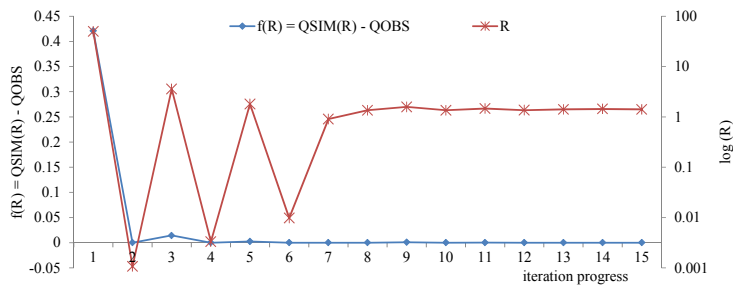


Figure 32: Illustration of the iteration progress for one model time step. Note that the right y-axis showing the inverse rainfall values (R) is in a logarithmic scale.

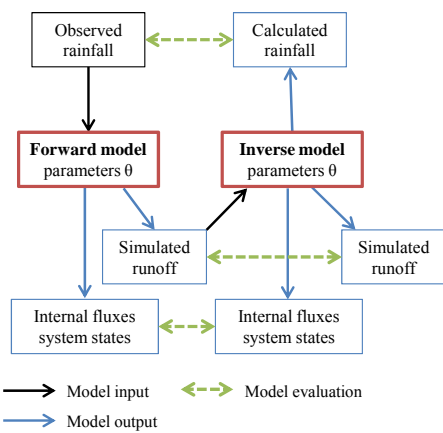


Figure 43: Setup of the virtual experiments and evaluation of the inverse model. All variables are calculated for every Monte Carlo run, in which parameters θ are varied.

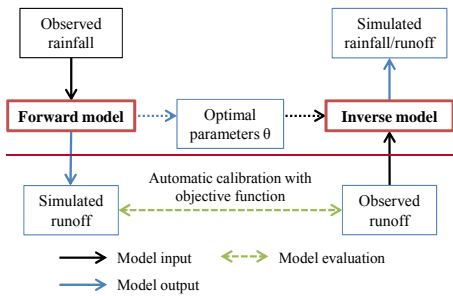
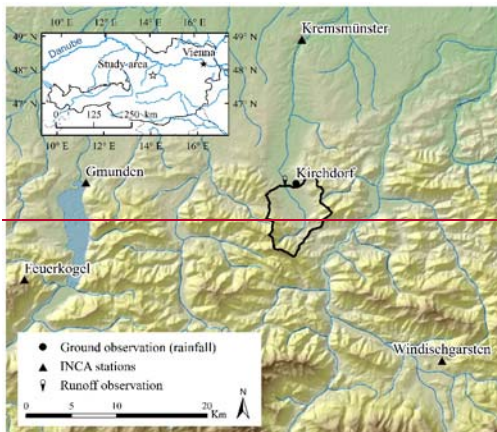


Figure 5: Parameter estimation and calculation scheme.



Formatiert: Englisch (Großbritannien)

Formatiert: Englisch (Großbritannien)

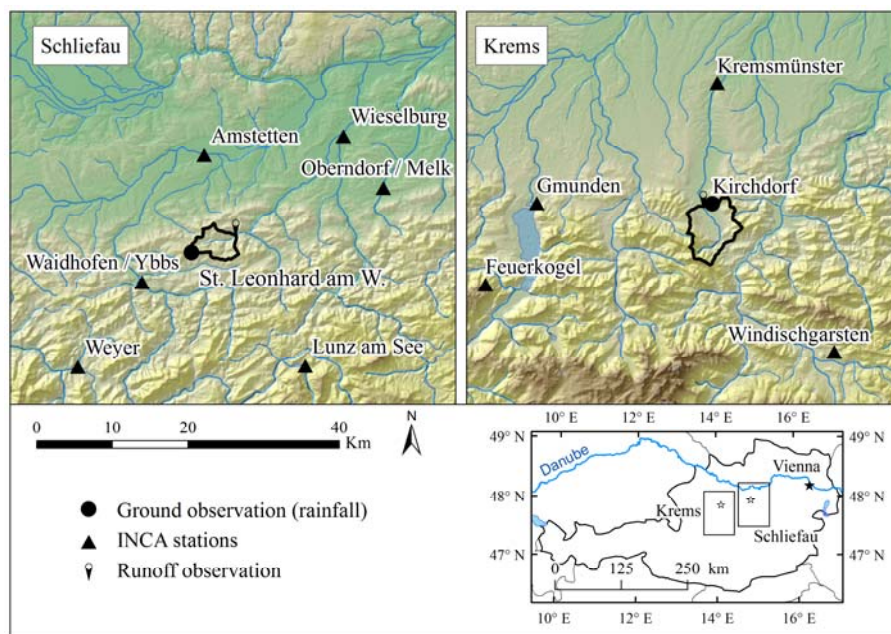


Figure 654: Schlieffau and Krems catchment and location of meteorological stations. Note that ground observation of rainfall is not part of the INCA stations network.

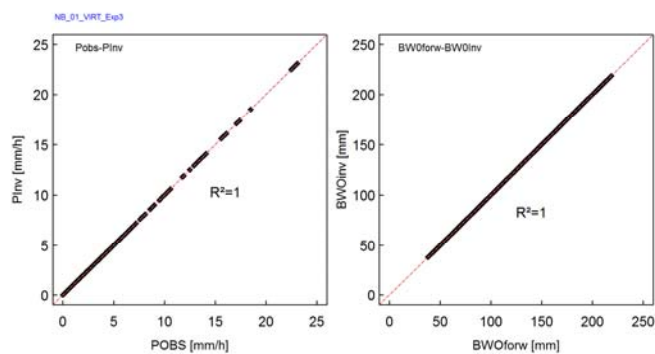


Figure 65: Virtual experiment with simulated runoff as input into the inverse model (Schlieffau catchment): Identical observed and inverse rainfall (POBS-PInv, left) and soil water content of forward and inverse model (BW0forw-BW0Inv, right).

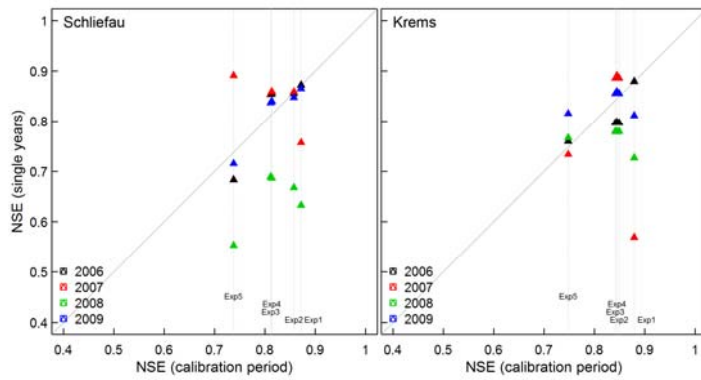


Figure 76: Nash-Sutcliffe-Efficiency (NSE) of the forward model for the calibration periods versus single years for the 2 study areas.

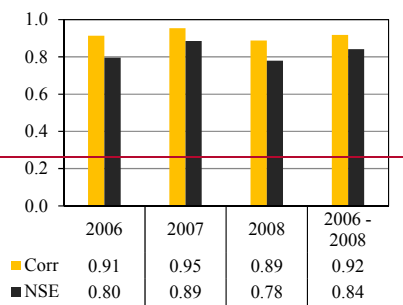


Figure 7: Model performance for the calibration period expressed by correlation (CORR) and Nash-Sutcliffe Efficiency (NSE)

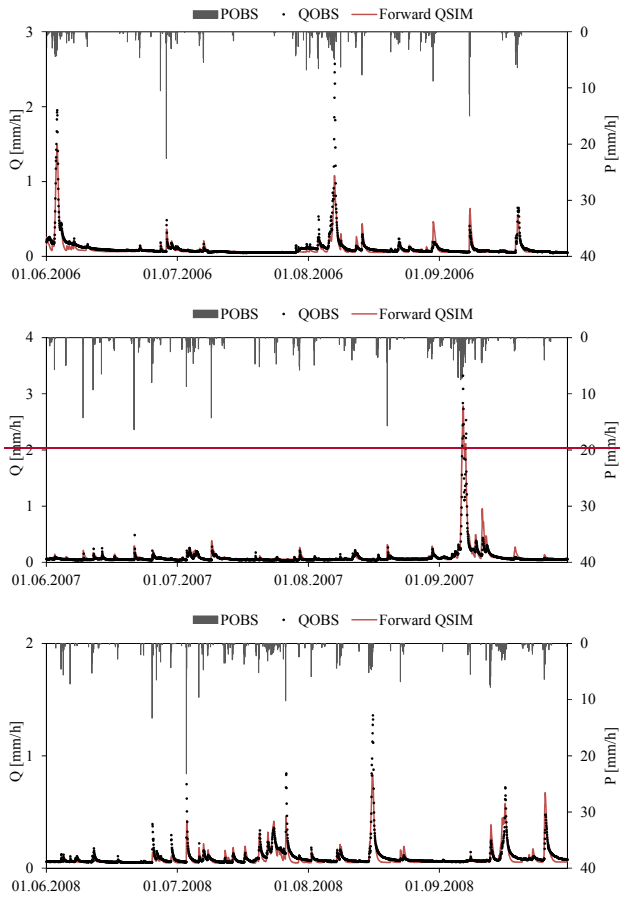


Figure 8: Observed (QOBS) and simulated runoff of the forward model (Forward QSIM) for the calibration periods. Ground observation of rainfall (POBS) used as input is also shown

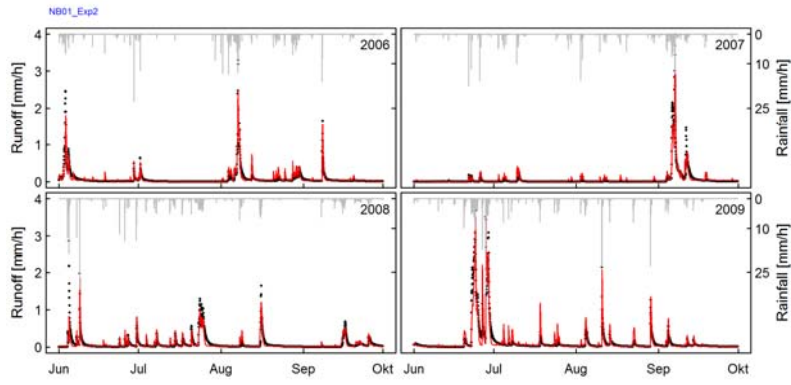


Figure 87: Schlieffau catchment: Observed (black points) and simulated (red) runoff of Exp2.

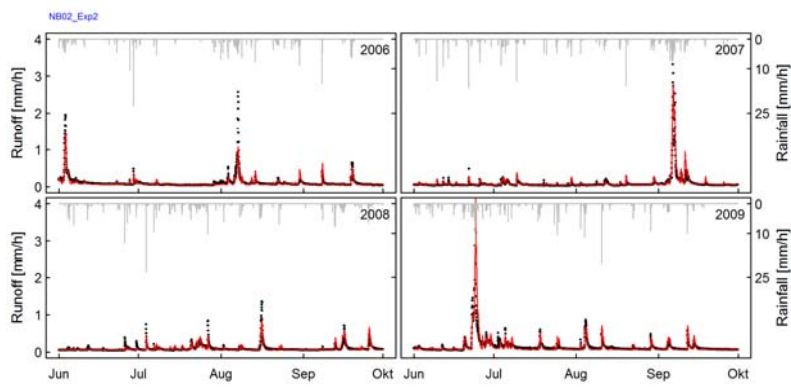
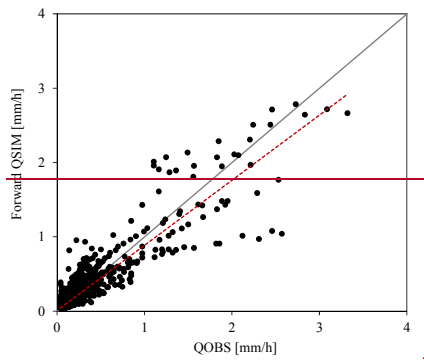


Figure 98: Krems catchment: Observed (black points) and simulated (red) runoff of Exp2.

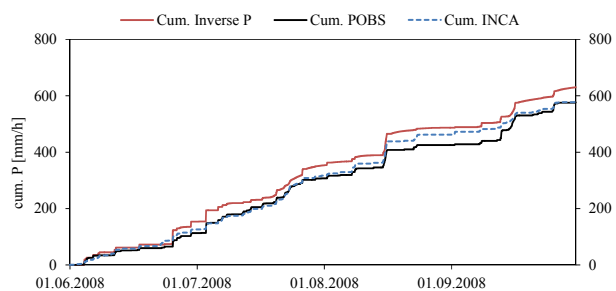
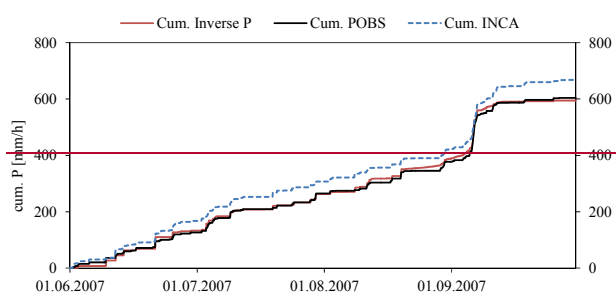
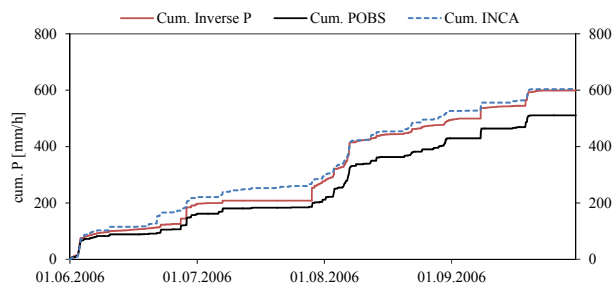
1330
1331



1332
1333
1334
1335

Figure 9: Scatterplot between observed (QOBS) and simulated runoff (Forward QSIM) for the calibration period, including the dotted regression line

Formatiert: Englisch (Großbritannien)



Formatiert: Englisch (Großbritannien)

1336

1337

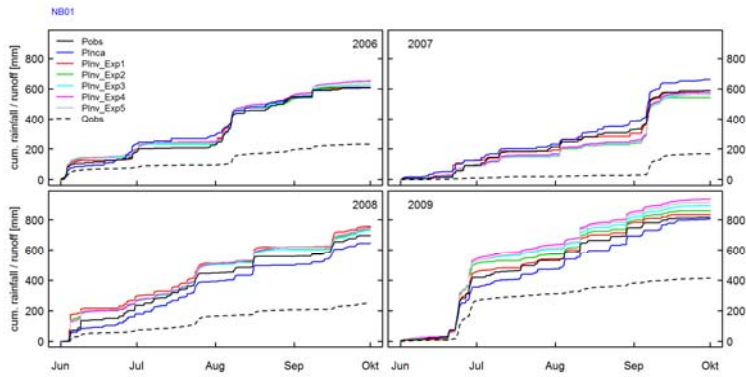


Figure 140: Schliefauf catchment: Cumulative rainfall curves for ~~inverse~~, observed rainfall (POBSbs), and INCA rainfall (PInca) and the inverse rainfall of Exp1 to Exp5 (PInv). Cumulative sums of observed runoff are shown ~~also~~ as dashed black lines. ~~shown.~~ for the periods in 2006, 2007 and 2008

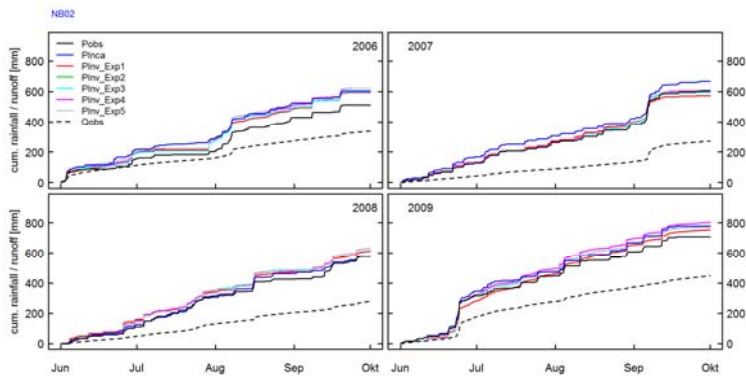


Figure 140: Krems catchment: Cumulative rainfall curves for observed rainfall (POBSbs), INCA rainfall (PInca) and the inverse rainfall of Exp1 to Exp5. Cumulative sums of observed runoff are shown as dotted black lines. Cumulative sums of observed runoff are also shown.

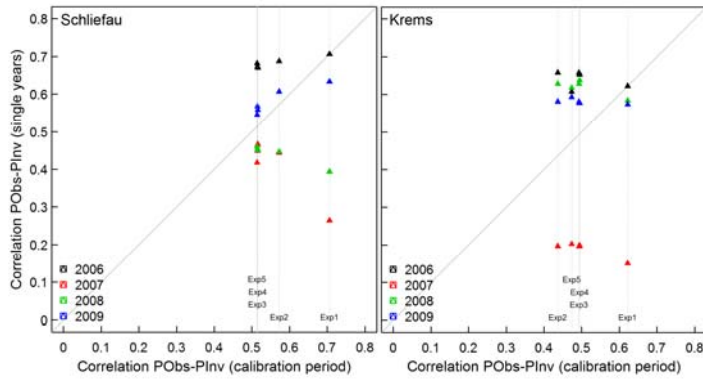


Figure 121: Correlation between PObs-PInv for the calibration periods of the simulation experiments Exp1 to Exp5 and versus single years for the 2 study areas.

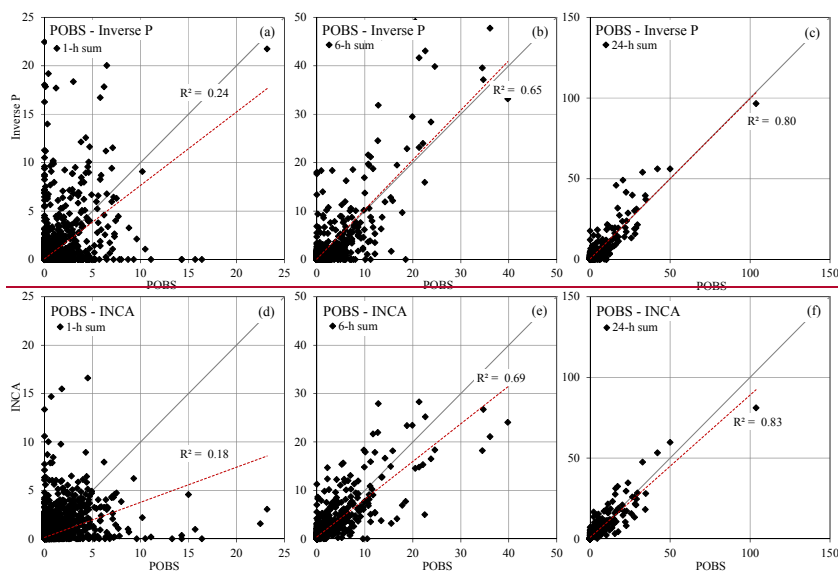
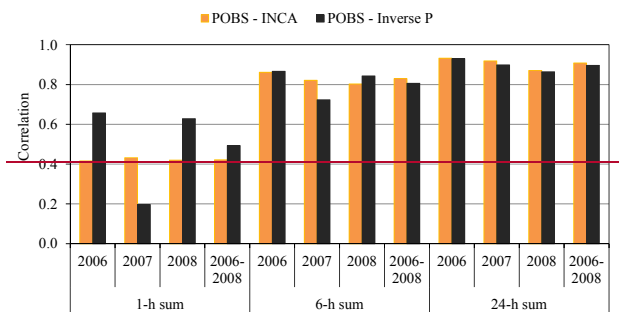


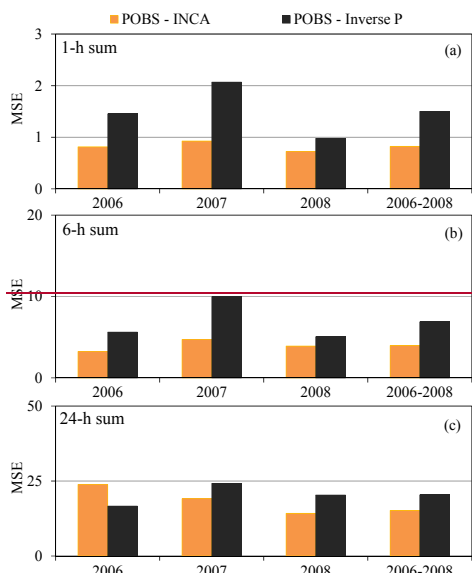
Figure 11: Scatterplot between station data (POBS) and inverse rainfall (Inverse P) (upper row) and INCA data (lower row) for 1-h, 6-h and 24-h sums

Formatiert: Englisch (Großbritannien)



Formatiert: Englisch (Großbritannien)

Figure 12: Correlation between different rainfall realisations and for different evaluation periods and temporal aggregation lengths



Formatiert: Englisch (Großbritannien)

Figure 13: Mean-squared error (MSE in $(\text{mm/h})^2$) between different rainfall realisations and temporal aggregation lengths

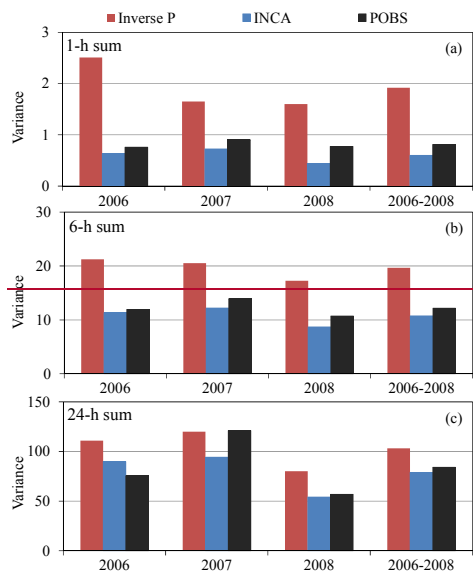
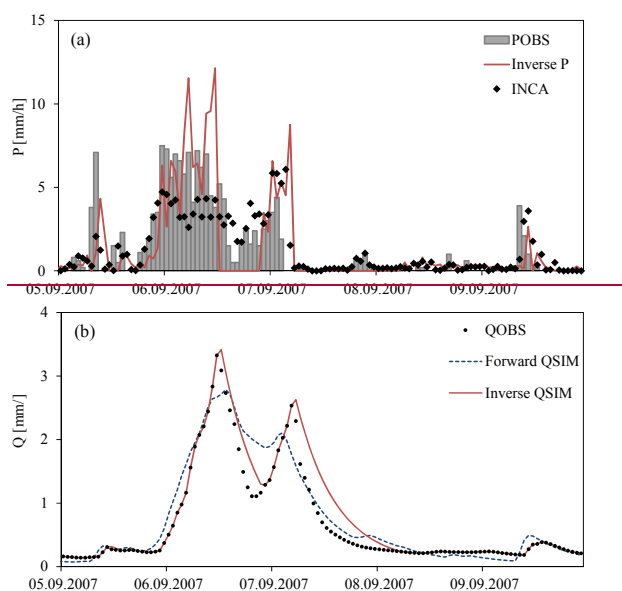
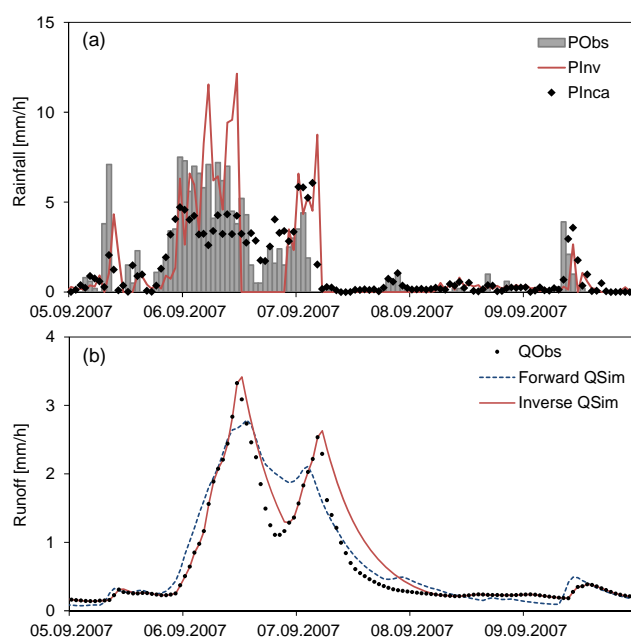


Figure 14: Variance for different rainfall realisations and temporal aggregation lengths

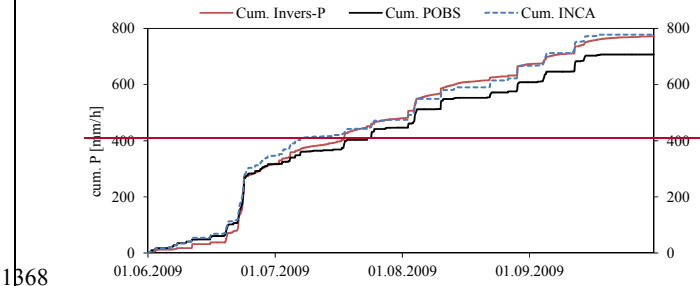
1364



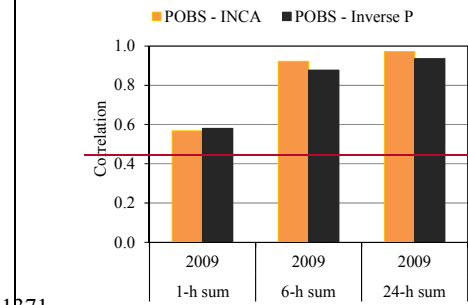
1365



1366 Figure 4512: Krems catchment: Temporal development of the different rainfall realisations
1367 (a) and runoff (b) for a flood event. Simulations originate from Exp3.



1369 ~~Figure 16: Cumulative rainfall curves for inverse, observed and INCA rainfall for the~~
1370 ~~independent period in 2009~~



1372 ~~Figure 17: Correlation between different rainfall realisations in the independent validation~~
1373 ~~period 2009 and temporal aggregation lengths~~

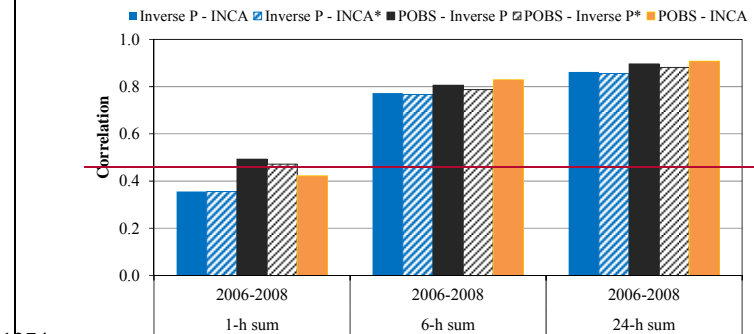
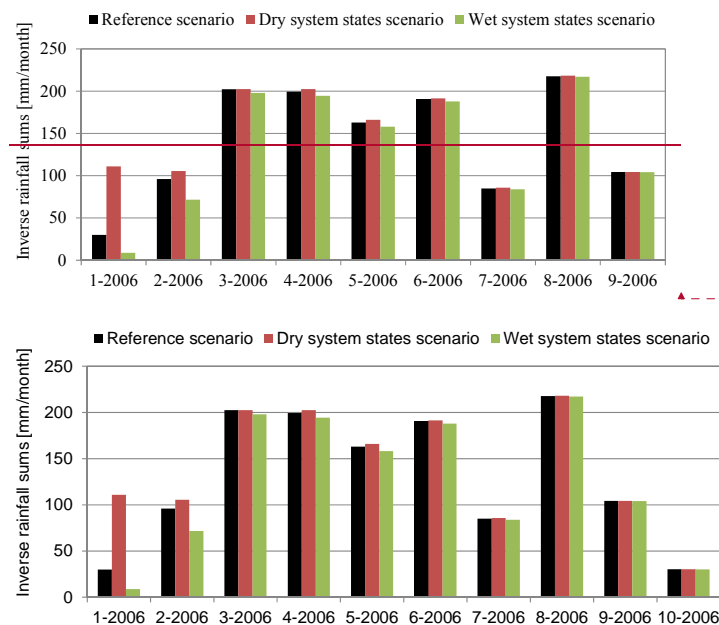


Figure 18: Correlation between different rainfall realisations and temporal aggregation lengths. Data marked with an asterisk (*) is based on the calibration with INCA data as input



Formatiert: Englisch (Großbritannien)

Formatiert: Englisch (Großbritannien)

Figure 19: Krems catchment: Monthly sums of inverse rainfall simulated in the scenarios "reference", "dry" and "wet" from Exp6.

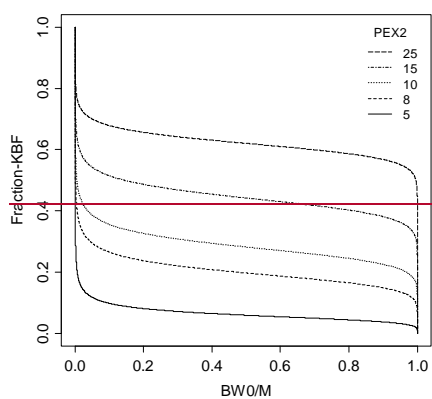


Figure A1: Fraction of parameter KBF as a function of relative soil water content (BW0/M) and the parameter PEX2

